

NASA CR-156658

NASA CR-
ERIM 118500-1-F



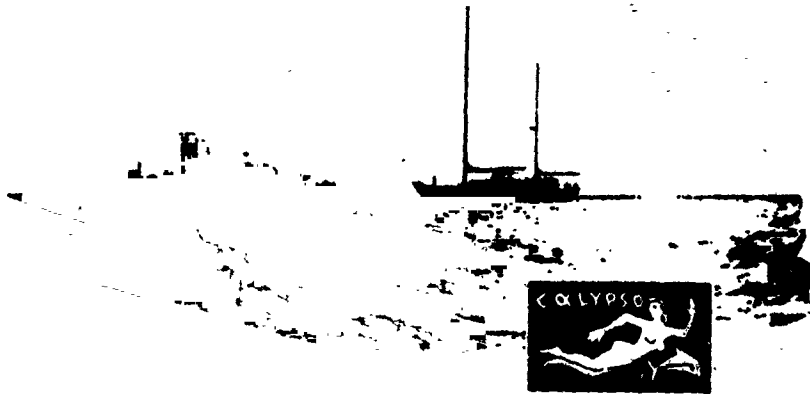
Final Report

NASA/COUSTEAU OCEAN BATHYMETRY EXPERIMENT

Remote Bathymetry Using High Gain LANDSAT Data

FABIAN C. POLCYN
Infrared and Optics Division

JULY 1976



Prepared for
NATIONAL AERONAUTICS AND SPACE ADMINISTRATION

Goddard Space Flight Center
Greenbelt, Maryland 20771
Contract NAS5-22597
Technical Monitor - Charles Bohn

**ENVIRONMENTAL
RESEARCH INSTITUTE OF MICHIGAN**
FORMERLY WILLOW RUN LABORATORIES, THE UNIVERSITY OF MICHIGAN
BOX 618 • ANN ARBOR • MICHIGAN 48107

(NASA-CR-156658) NASA/COUSTEAU OCEAN
BATHYMETRY EXPERIMENT. REMOTE BATHYMETRY
USING HIGH GAIN LANDSAT DATA Final Report, Aug. 1975 - Apr. 1976 (Environmental
Research Inst. of Michigan) 132 p

G3/48 01175
Unclass

N78-15662
AD/MP AD1



TECHNICAL REPORT STANDARD TITLE PAGE

1. Report No. NASA-CR-ERIM-118500-1-F		2. Government Accession No.		3. Recipient's Catalog No.	
4. Title and Subtitle NASA/COUSTEAU OCEAN BATHYMETRY EXPERIMENT REMOTE BATHYMETRY USING HIGH GAIN LANDSAT DATA				5. Report Date JULY 1976	
				6. Performing Organization Code	
7. Author(s) Fabian C. Polcyn				8. Performing Organization Report No. 118500-1-F	
9. Performing Organization Name and Address Environmental Research Institute of Michigan P.O. Box 8618 Ann Arbor, Michigan 48107 (313) 994-1200, Ext. 234				10. Work Unit No.	
				11. Contract or Grant No. NAS5-22597	
				13. Type of Report and Period Covered Final Report August 1975-April 1976	
12. Sponsoring Agency Name and Address National Aeronautics and Space Administration Goddard Space Flight Center Greenbelt, Maryland 20771				14. Sponsoring Agency Code	
15. Supplementary Notes					
16. Abstract <p>Satellite remote bathymetry was successfully verified to 22 m depths where water clarity was defined by $\alpha = .058 \text{ m}^{-1}$ and bottom reflection, r_b, was 26%. High gain Band 4 and Band 5 CCT data from Landsat-1 was used for a test site in the Bahama Islands and near Florida.</p> <p>Near Florida where $\alpha = .11 \text{ m}^{-1}$ and $r_b = 20\%$, depths to 10 m were verified. Depth accuracies within 10% rms were achieved. Position accuracies within one Landsat pixel were obtained by reference to the Transit navigation satellites.</p> <p>Two ships, Calypso and Beayondan, were at anchor on each of the seven days during Landsat-1 and 2 overpasses: LORAN-C position information was used when the ships were underway making depth transects. Results are expected to be useful for updating charts showing shoals hazardous to navigation or in monitoring changes in nearshore topography.</p>					
17. Key Words Landsat shoal detection charting multispectral scanner computer processing			18. Distribution Statement Initial distribution is listed at the end of this document.		
19. Security Classif. (of this report) Unclassified		20. Security Classif. (of this page) Unclassified		21. No. of Pages 132	22. Price



PREFACE

This report presents the results of an experiment in remote bathymetry conducted jointly as a NASA/Cousteau Society Ocean Bathymetry experiment in August and September of 1975. Fabian C. Polcyn, Senior Research Engineer of the Environmental Research Institute of Michigan, served as Principal Investigator. Many personnel from several organizations participated in the preparation and execution of the experiment. Among these are:

*Cousteau Society

Captain Jacques Cousteau, Experiment Co-Sponsor

*NASA Headquarters

Mr. Russell Schweickart, Experiment Coordinator

*NASA Goddard

Dr. Enrico P. Mercanti, Experiment Manager

Mr. Charles Bohn, Experiment Manager and Technical
Monitor

Dr. Ross McCluney, Experiment Scientific Monitor

Mr. Charles Vermillion, NASA/Calyпсо Coordinator

Dr. John Barker, Real Time Landsat Processing

Mr. Locke Stuart, Experiment Advisor

Mr. Albert Whalen, ATS-3 Communications

*Texas A&M

Mr. John M. Hill, Oceanographer and Whiting Study Coordinator

*John Hopkins University

Mr. Edward Westerfield, Transit and LORAN-C

Mr. Dan Mitola, Beyondan Coordinator

*U.S. Coast Guard

Charles Montanese, LORAN-C

Robert Riper, LORAN-C

*Defense Mapping Agency

Jim Hammack, Historical Data and Navigation Charts

Dennis Granato, LORAN-C Grid Conversion

Because of the wide scope of the experiment, separate reports are being prepared related to the different aspects of the experiment, e.g., real time data processing performed at NASA, Goddard by Dr. John Barker and accurate position information obtained by Johns Hopkins University under the direction of Mr. Ed Westerfield. This report focuses on the remote bathymetry aspects of the experiment.

A special note of appreciation is given to experiment managers Enrico Mercanti and Charles Bohn for their tireless efforts in bringing together, under a tight time schedule, the several elements to ensure the successful completion of the experiment.

Acknowledgement is given to Charles Vermillion, John M. Hill, Rusty Schweickart, and Jack Ford for their support, cooperation and participation in the shipboard data collection phase of the experiment.

Particular thanks to Jacques Cousteau and the crew of the Calypso for their dedication and expertise in the underwater phases of the experiment, without which, measurements of key experimental parameters could not have been made.

Special thanks to Dan Mitola and Ed Westerfield and the crew of the Beayondan for their patient efforts in obtaining the accurate position information, without which, verification of the calculated depths with the measured depths would have been difficult.

At ERIM, the collaboration of Dr. David R. Lyzenga in model development and computer analysis of the high gain Landsat data tapes is gratefully acknowledged.

This report was reprinted after minor corrections were made in July 1977. Pages 44 through 127 were repaginated.



CONTENTS

1. INTRODUCTION 9
 1.1 Scope of Study
 1.2 Approach
 1.3 Summary of Conclusion

2. PREVIOUS WORK 13

3. DESCRIPTION OF EXPERIMENT 14
 3.1 Outline of Experiment
 3.2 Shipboard Operation
 3.3 Data Preparation

4. CALCULATION OF WATER DEPTH 31
 4.1 Model Development
 4.2 Comparison of Calculated vs Measured Depth
 at Station F-1
 4.3 Extension of the Calculations to Other Areas
 4.4 Extension of the Calculations to Another Date
 4.5 Saturation of Band 4 and 5

5. DEPTH CALCULATIONS NEAR THE FLORIDA COASTLINE 54

6. CONCLUSION 61

REFERENCES 64

APPENDIX A: TECHNICAL MEMORANDUM S3R-76-067 65

APPENDIX B: TECHNICAL MEMORANDUM RSC-131 95

DISTRIBUTION LIST 132

LIST OF ILLUSTRATIONS

<u>Figure</u>	<u>Title</u>	<u>Page</u>
1	Bahama test site for four consecutive Landsat Passes	15
2	Cousteau at recording fathometer	17
3	Ship transect defined by LORAN-C	18
4	Submarine multichannel photometer	20
5	Diver measuring light reflected from calibrated gray scale	22
6a	Three step calibrated gray scale made specially for experiment	23
6b	Two 35 mm lens Nikonos cameras filtered to match Band 4 and Band 5 of Landsat-1 and 2	24
7	Transmissometer deployed underwater to measure beam attenuation of water	26
8	Green and red band transmission versus water depth	27
9	Band 4 filtered images	30
10	Bathymetry map made from Band 4	33
11	Landsat-1 calculated depth vs measured depth	38
12	Landsat-1 calculated depth based on October 12, 1975 data	41
13	Bathymetry map from Landsat-1, Band 4, October 12, 1975 with overlay from Chart N.O. 26320	45
14	Bathymetry map from Landsat-1, Band 4, October 12, 1975 with overlay from Chart N.O. 26320, Data averaged over 6x6 resolution elements	47
15	Bathymetry map from Landsat-1, Band 4, October 12, 1975 with overlay from Chart N.O. 26320, data averaged over 6x6 resolution elements	49

<u>Figure</u>	<u>Title</u>	<u>Page</u>
16	Saturation depths from Landsat-1 Bands 4 and 5 . . .	51
17	Bathymetry map from Landsat-1, Band 5, October 12, 1975	52
18	Signal-related depth profile near Florida coastline	57
19	Satellite calculated depth profiles for two transects near Hollywood, Florida	58
20	Color coded depth map made from Landsat image . . .	60
21	Signal difference versus band position (Landsat-D)..	63

LIST OF TABLES

<u>Table</u>	<u>Title</u>	<u>Page</u>
1	NASA/Cousteau Bathymetry Experiment, August/ September 1975	17
2	Average water attenuation coefficients derived from photometer data Bahamas and Florida 1975	28
3	Average MSS 4 signals observed over deep water, September 6, 1975.	37
4	Average MSS 4 signals over deep water, October 12, 1975, Landsat-1	40
5	Color code for depth range of Florida coastline map	60

REMOTE BATHYMETRY USING
HIGH GAIN LANDSAT DATA

1

INTRODUCTION

This report prepared under contract NAS5-22597 gives the remote bathymetry results obtained as part of the NASA/Cousteau Ocean Bathymetry Experiment. This experiment using the high gain mode of both Landsat 1 and Landsat 2 was conducted between August 21 and September 8, 1975 with the test site centered in the Bahama Islands. Analysis of Landsat CCT data took place between October 1975 and April 1976.

Two ships, Calypso and Beayondan and thirteen satellites were used in the experiment in order to obtain the necessary supporting data and position verification. The results are expected to be useful in the preparation of charts in order to update the location of hazardous shoals and to monitor changes in nearshore underwater profiles resulting from storm and wave action.

1.1 SCOPE OF STUDY

Previously, the International Hydrographic Office defined shoals as hazardous to shipping if they fell in the range from 0 to 17 meter depths. With the advent of supertankers, the need to "clear" the shipping lanes to 25 and 30 meter depths becomes a serious concern in order to help prevent accidents and thus avoid potential oil spills from affecting the environment. More accurate charts could lead to savings in ship transportation costs by reducing time spent on unnecessary routes to avoid uncertain shoals.

Not all countries of the world have the necessary ship resources to provide the type of measurements needed to update charts in

their areas. In order to determine the role of satellite remote sensing in helping to provide usable information to alleviate this problem, this experiment was conducted to answer two specific objectives:

1. What is the maximum depth measurable using high gain data from Landsat 1 and 2 (in particular, for Band 4 whose wavelengths have the best clear water penetration capability of the 4 channels available on Landsat 1 and 2)?
2. What is the accuracy of the depth measurement made using satellite data combined with suitable supporting ground data?

If practical values could be derived from satellite remote bathymetry than a comparatively rapid means for surveying the critical ocean areas would be created.

The experiment also included a demonstration of a possible future satellite to ship data communication system wherein satellite imagery could be relayed directly to a ship on the same day of its collection giving that ship the most recent information on potential hazards over a large area. Since one frame of Landsat data covers a 100 nm square, a ship traveling at 10 knots would be given a maximum of 10 hours of travel time over which current information would be available. With two satellites in orbit, 9 day old information is theoretically achievable for any part of the globe, provided a rapid means for processing the data is perfected. The real time processing of Landsat data (completed on the same day that the image was formed) and transmission of depth contour data to the Calypso that was successfully demonstrated during this experiment is the subject of a separate NASA report.

If cloud cover lessens the chance for the full realization of this concept, the repetitiveness of the satellite coverage does suggest the possibility of some type of chart updating at intervals shorter than now available. In certain parts of the world charts may be anywhere from 10 to 100 years old because of the lack of ship and money resources to complete surveys at shorter intervals. If practical depths are measurable at acceptable accuracies, the cost savings in equivalent ship survey time could be substantial.

1.2 APPROACH

Remote bathymetry takes advantage of two characteristics. Water selectively absorbs different wavelengths of light, and energy at each wavelength is strongly absorbed as a function of the depth of the water. As the sun's energy penetrates the ocean, losses occur (1) at the surface, (2) through the water column, (3) at the reflection from the bottom, then (4) through the water column for the return path, (5) at the surface again, and finally (6) through the atmosphere to the satellite where it is collected by multispectral scanner in selected wavelength bands. By knowing the sensor sensitivity calibration and taking each parameter into account, the MSS voltages expressed digitally can be used to calculate the depth of water. Two variables had to be measured at the time of the satellite overflight. The first was the light absorption of the water in the same bands in which the satellite sensor operates, and the second was the percent reflection of the bottom surface. The experimental team aboard the "Calypso" made the necessary submarine photometer, transmissometer, and reflectance measurements at several sites during the satellite overpasses.

The Calypso made a number of transects to record fathometer depths so that satellite-derived depths could be checked against ship measurements. The team aboard the "Beayondan" operated by the Applied Physics Laboratory of John Hopkins University provided accurate location information using LORAN-C and TRANSIT navigation satellite fixes. LORAN-C measurements aboard the Calypso were also used for position information and the ship's transects were correlated with Beayondan measurements at a number of rendezvous points. During the time of the satellite overpass, both ships were anchored side-by-side so that later, the depth measured by the MSS at the corresponding Landsat CCT pixel containing the ship could be correlated with actual depth as measured by a fathometer.

Twelve land points subsequently were used to convert line and point elements of the Landsat CCT to geographical coordinates.

1.3 SUMMARY OF CONCLUSIONS

Supported only by measurements of average water transmission and bottom reflection data, high-gain Landsat Bands 4 and 5 were used to construct bathymetry maps of test areas near the Berry Islands and near Hollywood, Florida. Depths to 22 m were reliably verified at accuracies within 10% (rms) of measured values at the site West of the Berry Islands where water transparencies of 0.05 m^{-1} and 26% bottom reflections were encountered. CCT signals two digital counts above deep water signals were identified to be caused by light reflected from 40 m depths. Landsat data taken in October over the same site successfully gave the same depths (within the same accuracies) as the depths derived using September data, when both satellite data and water characteristics were measured on the same day.

Depths to 10 m were verified at the Florida site where water was less transparent with $\alpha = .11 \text{ m}^{-1}$ and bottom reflectance equal to 20%.

At 3x gain for Landsat 1, Band 4 was found to saturate at 1.3 m depths and Band 5 saturated at 0.3 m depth for high reflective bottom (about 30% in Band 4). Thus Band 5 can be used to cover the range where Band 4 reaches saturation.

For an area with uniform average characteristics both in time and space as seen by the integration over each resolution element, the knowledge of point characteristics can be extended to the larger area. Alternative ground supporting data such as knowledge of specific water depths at two or more control points for each combination of water clarity and bottom types would serve equally well.

Cloud free scenes should be used to avoid spurious shallow anomalies resulting from partial cloud cover or from cloud reflections of sunlight from the ocean surface.

PREVIOUS WORK

The general technique for remote bathymetry was first tested using aircraft multispectral data [1]. Two-channel techniques were explored to reduce the dependency on the knowledge of the absolute values of bottom reflection and water transmission characteristics. Two-channel processing was employed in an ERTS-1 experiment [2]. In that work, the two-channel data gave results to 3 m. At this depth, the signal from Band 5, which operates where water more strongly absorbs, is the limiting factor. Channel 4 data, however, was usable to 9 m depths using normal-gain Landsat data.

The high-gain Landsat data used in this experiment provides a better digitization of signal range encountered from sites with varying depths. With a wider range of signal spread over more digital values, each digital step represents a finer depth increment so that two advantages are achieved. First, depth values can be measured within finer bounds with less ambiguity. Second, deeper depths can be measured. Two or three digital values above the mean deep water background signal (with a standard deviation of less than 2 counts) can, in some cases, be interpreted as evidence of the presence of the ocean bottom (see Chapter 4).

Future sensors should be made to operate in bands closer to the optimum transmission of water. An investigation of the optimum placement for future satellite MSS channels for water depth measurements is reported in [3].

DESCRIPTION OF EXPERIMENT

The experimental team met in Nassau, New Providence Island, between August 21 and August 25, 1975 to complete preparations. LORAN-C equipment was installed on the Calypso with the assistance of Charles Montanese and Robert Riper of the U.S. Coast Guard. Instruments manufactured by Kahl Scientific Instrument Corporation for measuring water transparency and bottom reflections were transferred to the Calypso at this time and a trial run took place near the island on August 26, 1975 to familiarize the team with the experimental procedures.

3.1 OUTLINE OF EXPERIMENT

The plan of the experiment called for the two ships, Calypso and Beayondan to be on station during the Landsat-2 overpass on four consecutive days (August 27, 28, 29, and 30, 1975). The sequence was to be repeated for Landsat-1 on September 5, 6, 7, and 8, 1975. On August 27, the first day on station, the rendezvous point was north of Eleuthera Island. By sailing 90 nm westward during the night (see Figure 1), the two ships were able to be in position the following day for a Landsat overpass, west of the Berry Islands on the northern edge of the Great Bahama Bank. This site was considered our prime test area. It was chosen because of its gradual change in depth from one meter of water to deep ocean water in a north and south span of 25 nm. Laterally to this slope, it is relatively uniform so that a broad incline of ocean bottom is available for investigating the maximum water depths detectable from a satellite. At the same time it enables the depth accuracy to be determined with precision. It also makes the exact knowledge of the ship's position less critical during subsequent data analysis efforts, should the position accuracy

ORIGINAL PAGE IS
OF POOR QUALITY

Landsat-2	Aug 30	Aug 29	Aug 28	Aug 27
Landsat-1	Sept 8	Sept 7	Sept 6	Sept 5
Center of Pass	4	3	2	1

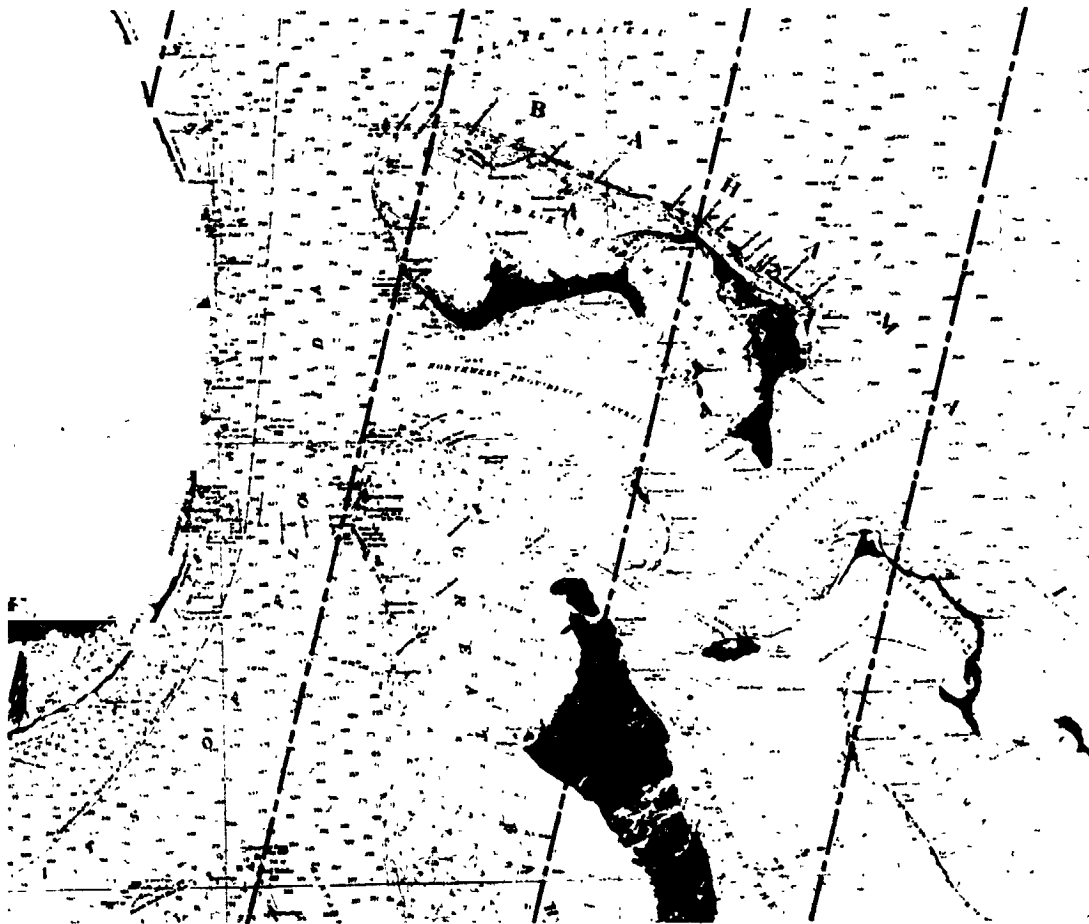


FIGURE 1. BAHAMA TEST SITE FOR FOUR CONSECUTIVE LANDSAT PASSES.

of a given depth measurement be in doubt within one or two picture elements. The water clarity and relatively uniform bottom reflectance at this site also permitted the goal of the experiment to be better achieved.

Table 1 lists the station locations, where underwater measurements were taken for each day of the experiment. At each station the Calypso and Beayondan were anchored so that accurate location information and depth soundings near each other are well correlated. The Beayondan would remain at these stations several hours in order to take advantage of the improved position accuracy obtainable from multiple passes of the six transit navigation satellites. These satellites fixes were then used to improve the LORAN-C position measurements.

During the time that the Beayondan obtained position information, the Calypso sailed at 8 knots along 10 to 15-mile linear transects, usually at a compass heading matching the ground track of Landsat. Along these transects fathometer data was obtained continuously with minute marks entered on the charts at the time that LORAN-C position data were also recorded (see Figure 2). The transects were also chosen so that sometime along the track, the Calypso would pass within 30 to 40 m (one half the size of a Landsat ground resolution element) of the anchored Beayondan. The time of passage and the range and bearing between the ships were taken into order to maintain correlation of depths measured with position (see Appendix A).

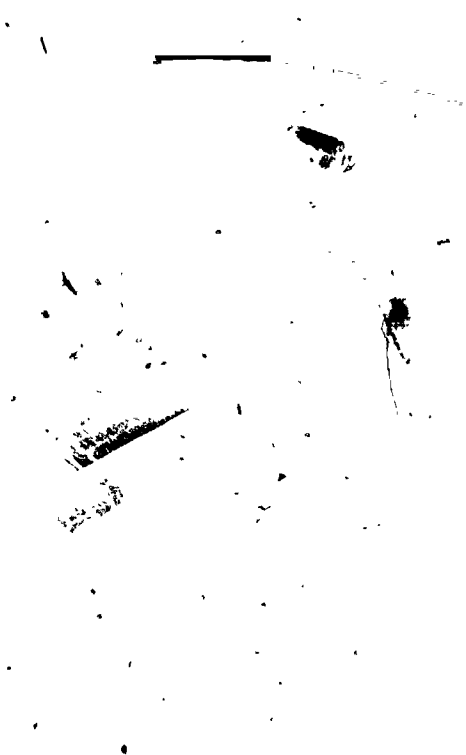
Between stations, the Beayondan also anchored near several landpoints to again check satellite position fixes with LORAN-C position information obtained from times of arrival differences in signals transmitted from a master station and two slave stations.

Figure 3 shows a typical ship transect defined by LORAN-C. It was taken on September 6 starting at 0425 EDT in the prime test site west of the Berry Islands. The positions are plotted at one or two minute intervals and were defined by converting the coordinates found by the LORAN-C time differences, to geographic coordinates from

TABLE 1
NASA/COUSTEAU OCEAN BATHYMETRY EXPERIMENT
AUGUST/SEPTEMBER 1975

TABLE OF STATIONS

DATE	STATION NUMBER	LOCATION
Aug 26		New Providence Island
Aug 27	A-1	North of Eleuthera Island
Aug 28	B-1	West of Berry Islands
Aug 28	B-2	West of Berry Islands
Aug 29	C-1	Little Issac
Aug 29	C-2	Great Issac
Aug 29	C-3	Great Issac
Aug 30	D-1	Hollywood, Florida
Sept 4	Transit	Little Bahama Bank
Sept 5	E(5)	Whiting Study
Sept 6	F-1	West of Berry Islands
Sept 7	F-2	Great Issac



ORIGINAL PAGE IS
OF POOR QUALITY

FIGURE 2. COUSTEAU AT RECORDING FATHOMETER. Deflection corresponds to depth while horizontal grid is minute by minute time marks for correlation with LORAN-C position information.

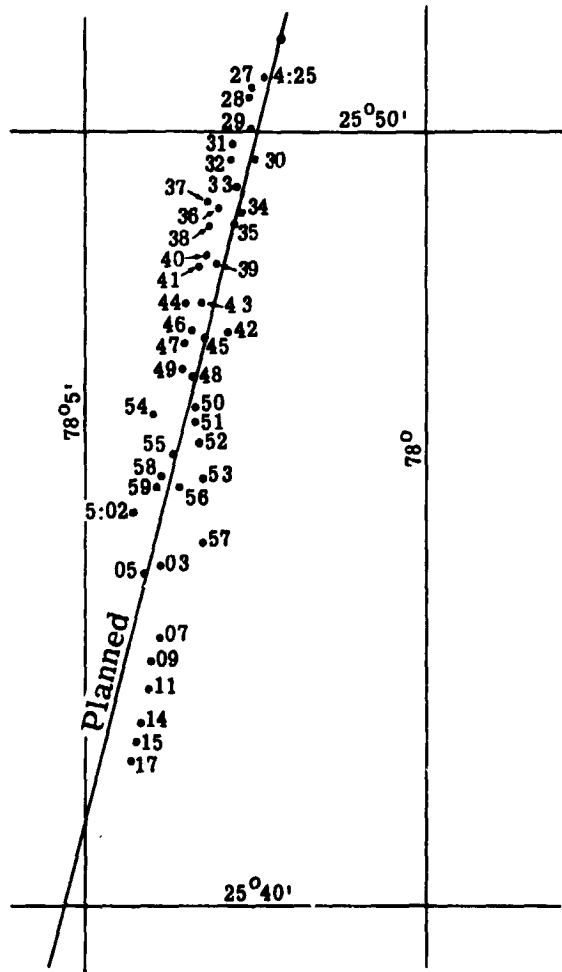


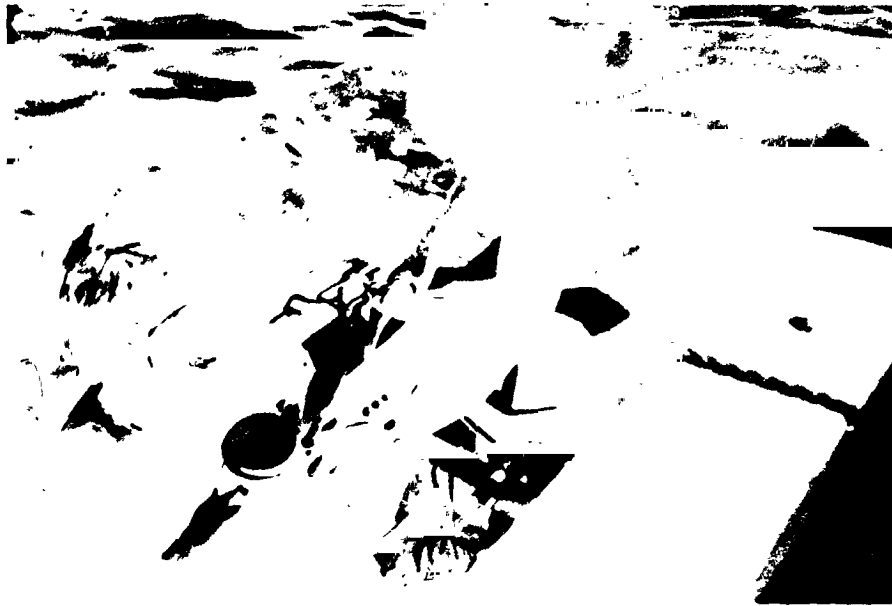
FIGURE 3. SHIP TRANSECT DEFINED BY LORAN-C
September 6 Tract Starts 0425 EDT
and Ends 0517 EDT.

maps supplied by the Defense Mapping Agency. The solid line is the planned heading. This part of the Atlantic lies at the fringe of the LORAN-C network, so that in some cases a poorly locked-on time difference gave a displaced apparent position of the ship. However, enough reliable points were obtained so that the ships average geographic position along the line could be determined.

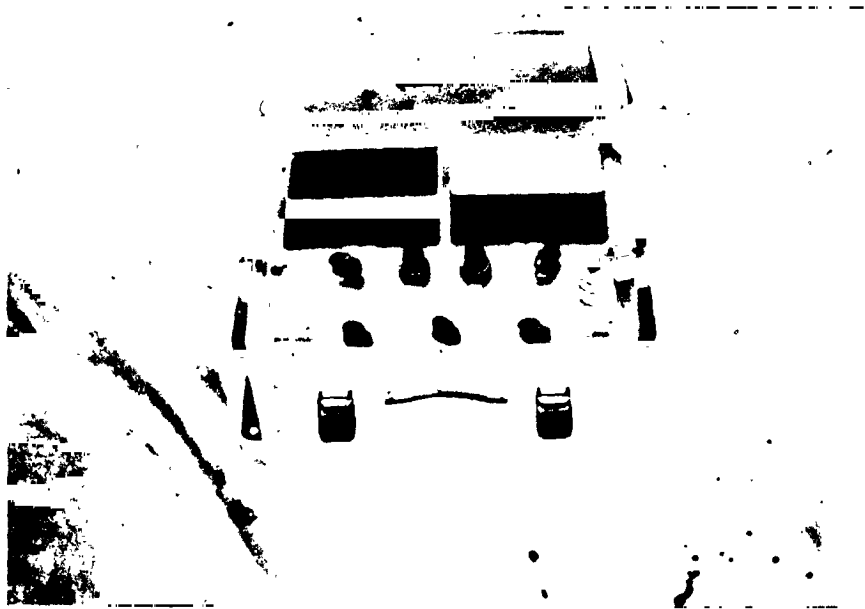
3.2 SHIPBOARD OPERATIONS

A series of underwater measurements was made at six of the anchored stations. Three types of instruments were employed to conduct these measurements. A multichannel submarine photometer, two filtered transmissometers and a combination of two Nikonos underwater cameras filtered to match Landsat Bands 4 and 5. The two cameras were used to photograph the ocean bottom; a 4-step calibrated reflectance gray scale was included in each frame. Three teams carried out the shipboard operations to obtain the necessary supporting water data. One team operated the multichannel submarine photometer (see Figure 4). This instrument consisted of two sensing cells and a deck control unit. One sensing cell, called a Deck Cell, remained on board ship fastened to the helicopter pad to get an unobstructed view of the sky. The Sea Cell, with four identical channels, was deployed away from the ship using 200-ft cables and lowered beneath the surface. Readings were made from both meters at the surface, and at selected depths of 1, 5, 10, and 15 m, as well as the bottom. At each level, the divers would hold the Sea Cell fixed, it always looked upward, integrating the light from the hemisphere above. During this moment, the team recording the radiance would cycle through the four detector positions. Two positions had filters which matched the Landsat Bands 4 and 5; the third was filtered for the blue region; and the fourth was unfiltered.

The necessary range selector adjustments were made each time, since less light reached the Sea Cell as it was lowered into deeper



(a) Sea cell being lowered into Zodiac for deployment 200 ft away from ship.



(b) Meters to read light reaching Deck Cell and Sea Cell in each of four detector positions.

FIGURE 4. SUBMARINE MULTICHANNEL PHOTOMETER.

water. At the same time that the Sea Cell detector positions were read, the corresponding Deck Cell detector readings were also recorded. In this way variations in the sun's illumination during the time between readings at different depths could be removed in the data reduction phase and only the effect of water depth on the light absorption would be determined.

The photometer data, by measuring the volume-integrated loss of energy as a function of water depth, gave values of the water extinction coefficient most suitable to the model which was used to compute water depth with the satellite CCT data. The photometer was also employed underwater in a second mode (see Figure 5). By restricting its field of view (a tube was attached underwater) the diver could obtain readings (again in all four spectral ranges) from each step of the calibrated gray scale as well as from typical surrounding bottom materials. From these data, the bottom reflectances in Bands 4 and 5 can be obtained if care in avoiding shadows is taken and no bottom sediment is permitted to be in suspension.

A second technique for accomplishing the same measurement used the two filtered Nikonos cameras. A three step gray scale panel with measured reflectances of 1%, 10.6%, and 29.6% (see Figure 6) was deployed underwater and photographed against the ocean bottom along with a secchi disk of known reflectance 84% to provide a fourth calibration step. Along with station location codes, the panels contained red and green stripes to code the black and white images so that no ambiguity would result later in determining in which spectral band an image was taken. By measuring the density of the negative across each gray level and then at selected points of the ocean bottom, an average percent reflectance of the bottom for that particular spectral band could be obtained. This parameter was also needed for the calculation of water depth. Different mixtures of bottom types were encountered at six sites during the experiment. Data from stations F-1 and D-1 were subsequently used to make detailed depth measurements.



FIGURE 5. DIVER MEASURING LIGHT REFLECTED FROM CALIBRATED GRAY SCALE.

ORIGINAL PAGE IS
OF POOR QUALITY



FIGURE 6a. THREE STEP CALIBRATED GRAY SCALE MADE SPECIALLY FOR EXPERIMENT. Station and Day Codes as well as color stripes for coding Nikonos Band 4 and 5 images were employed.



FIGURE 6b. TWO 35 mm LENS NIKONOS CAMERAS FILTERED TO MATCH BAND 4 AND BAND 5 OF LANDSAT 1 AND 2. Underwater exposures with Tri X film, ASA400 at f/11 at 1/125 sec for green band and f/5.6 at 1/125 sec for the red band were typical.

Two transmissometers were also used, each filtered so that beam attenuation measurements in spectral bands equivalent to Band 4 and 5 of Landsat could be made. They were lowered over the side of the Calypso (see Figure 7) and the percent light transmission from a light source through a fixed distance of water was measured. Measurements were made at 1, 5, and 10-m depths to check on the assumption of uniformity of the water column with respect to the average water transmission characteristics.

Special measurements were made and samples collected at Station E in the Little Bahama Bank in order to investigate the source of turbidity concentrations that appear in Landsat imagery and are sometimes mistaken for shallow water. The result of this phase of the investigation is given in Appendix B.

3.3 DATA PREPARATION - WATER ATTENUATION AND BOTTOM REFLECTANCE

The results of the submarine photometer work are summarized in Figure 8. In this graph, transmission of light, T , where $T = e^{-\alpha z}$, is plotted versus water depth, z . The attenuation coefficient α is usually expressed in m^{-1} . Data for both Band 4 (green) and Band 5 (red) are given for six stations. The transmission data were derived from the raw photometer data by comparing values in each band near the surface with each of the values measured at lower depths. This quotient was normalized by referring to the Deck Cell variations recorded at the same times as the Sea Cell data were obtained at the sequence of depths.

The average slopes of each of the lines of Figure 8 were then computed to produce the results given in Table 2. From this table, the variations in the type of water encountered at the six sites can be seen by an inspection of the values of α for Band 4. The clearest water $\alpha = 0.052 m^{-1}$, occurred at the Eleuthera test site, A-1 and theoretically, the deepest depths could be measurable there. The site F-1 west of the Berry Islands, measured on September 6, 1975, contained

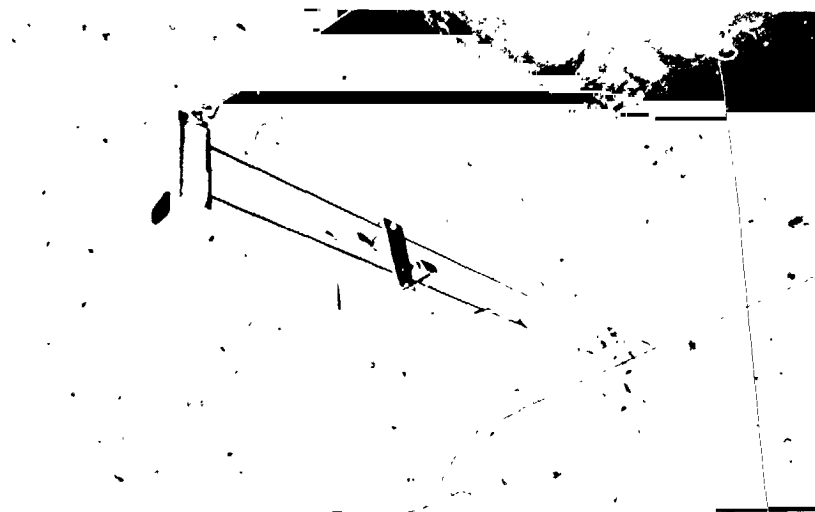


FIGURE 7. TRANSMISSOMETER DEPLOYED UNDERWATER TO MEASURE BEAM ATTENUATION OF WATER. Distance between light source and detector is adjustable and was typically set at 55 to 70 cm apart.

ORIGINAL PAGE IS
OF POOR QUALITY

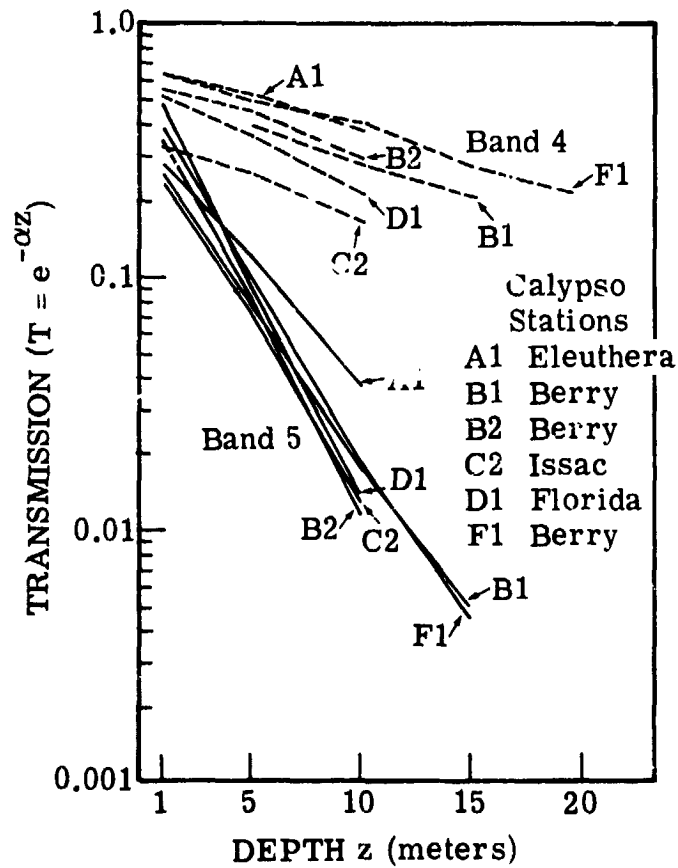


FIGURE 8. GREEN AND RED BAND TRANSMISSION VERSUS WATER DEPTH

TABLE 2
 AVERAGE WATER ATTENUATION COEFFICIENTS
 DERIVED FROM PHOTOMETER DATA
 BAHAMAS AND FLORIDA 1975

CALYPSO STATION		BAND 4 (m^{-1})	BAND 5 (m^{-1})
A-1	Eleuthera Aug 27	0.0522	0.219
F-1	Berry Sept 6	0.0586	0.314
B-1	Berry Aug 28	0.0638	0.273
B-2	Berry Aug 28	0.0661	0.369
C-2	Issac Aug 29	0.0748	0.326
D-1	Florida Aug 30	0.1067	0.374

the next clearest water $\alpha = 0.059 \text{ m}^{-1}$. The site D-1 near Florida, measured on August 30, 1975, had the poorest water clarity encountered, $\alpha = 0.107 \text{ m}^{-1}$.

The experimental test of satellite-measured water depth was performed for stations F-1 and D-1 in order to investigate the effect of changes in water attenuation on the maximum depth measurable. Consequently, the filtered Nikonos imagery of the gray scales for sites F-1 and D-1 (see Figure 9) were analyzed to compute the percent reflectance of the bottom. The corresponding photometer data taken at the same site gave comparable values.

Transmissometer data in the green band taken at station F-1 showed that the average percent transmission was of 88 ± 7 units over all depths measured. At D-1, the average percent transmission for all depths measured was 78 ± 5 units in the green band. Path was 55 cm in both cases.

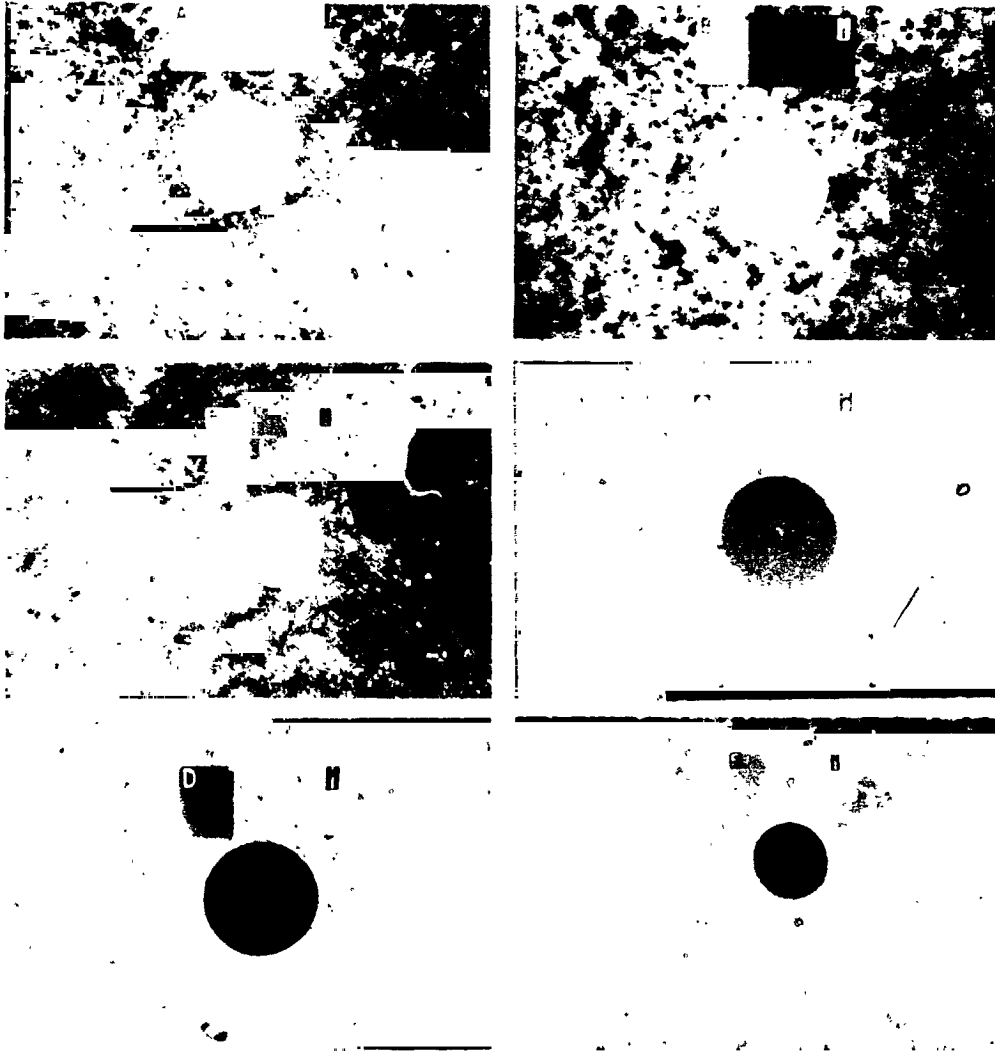


FIGURE 9. BAND 4 FILTERED IMAGES. Taken underwater at six locations with calibrated gray scale used to estimate percent reflectance of bottom.

CALCULATION OF WATER DEPTH

4.1 MODEL DEVELOPMENT

In order to compute water depth using remotely sensed signals, a relationship between signal voltage from the Landsat MSS and the depth of the water must be developed which includes the parameters that have an effect on the sun's energy as it passes through both the air and water paths and reflects from the ocean bottom. The complexity of the variables in this situation suggest that before a relationship can be developed, some simplifying assumptions are necessary. Three assumptions were made in this case. First, the model to be used would neglect scattering in the water. If we are investigating maximum depth penetration in clear water, this is not unreasonable. Secondly, we assume that the sensor signal comes only from direct solar radiation defined as E_0 . For the wavelengths in the green and red bands, this again is practical since skylight is dominated by blue wavelengths. The third assumption is placed on the property of α , the water attenuation coefficient, we assume it is independent of the radiance distribution for mathematical simplicity.

In general then, the voltage at the MSS output, V will be related to water depth, z , by the equation:

$$V = V_S + V_0 e^{-\alpha (\sec \theta + \sec \phi) z}$$

or
$$V = V_S + V_0 e^{-2\alpha z} \quad \text{for small values of } \theta \text{ and } \phi$$

where V_S = the signal level from deep water including atmospheric path. θ and ϕ are the refracted solar elevation angle and view angle respectively. ϕ is less than 5° while θ is less than 16°

and

$$V_0 = k_S \frac{T_1 T_2}{n^2} E_0 T \frac{r_b}{\pi}$$

such that k_s = Landsat-1 MSS 4 sensitivity constant
 T_1, T_2 = water surface transmittance (approximately 0.98)
 n = index of refraction = 1.33
 E_0 = surface irradiance
 $T = e^{-\tau}$, atmospheric radiance transmittance
 and r_b = bottom reflectance (assuming Lambertian reflection distribution).

Hence, if V_0 and α are known or can be calculated we can compute z by inspecting the Landsat signals after first subtracting the mean deep water signal. In a Landsat scene which covers 10,000 sq nm it does not prove difficult to find areas of deep water.

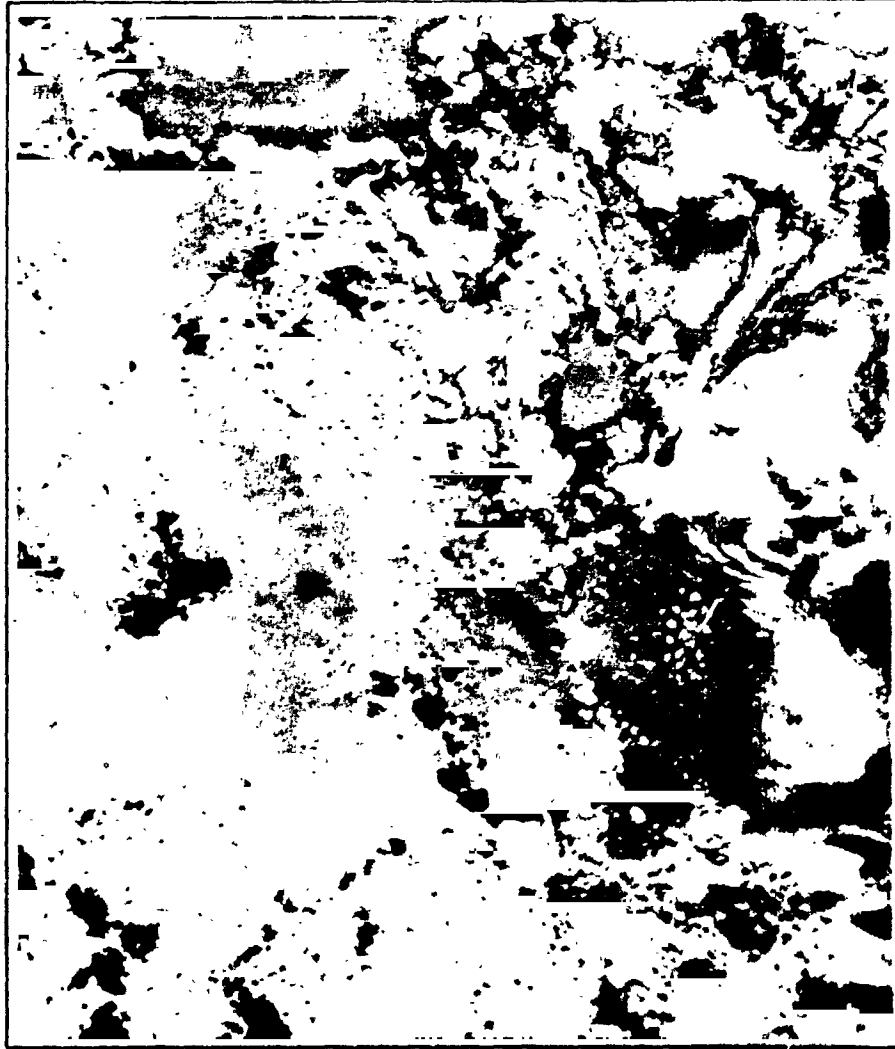
The water attenuation α was measured by the submarine photometer and is obtained from Table 2. Most of the terms in V_0 are constants or known parameters. The bottom reflectance r_b , was measured as described in section 3. E_0 , the surface irradiance was also obtained from the Sea Cell reading of the photometer at the surface. E_0 could also be obtained from knowledge of the sun's solar irradiance at the top of the atmosphere and modified by the atmospheric path transmission for a marine atmosphere. Finally, T was assumed to equal 0.8, the atmospheric radiance transmittance based on calculations of a Guttman-Kwajalein type atmosphere for this site [4].

4.2 COMPARISON OF CALCULATED DEPTHS FROM SATELLITE DATA VERSUS CALYPSO FATHOMETER READING AT STATION F-1

On September 6, 1975 at Station F-1 west of the Barry Islands, in the prime test area, Landsat-1 passed over the Calypso and Beayondan at about 10:30 EDT. The computer compatible tapes containing high gain data from this scene were subsequently used to construct a depth map (see Figure 10). The scene is partly cloudy, but the edge of the Great Bahama Bank is clearly delineated, as are several shallower depth ranges which were coded by printing in different colors. The digital



FORMERLY WILLOW RUN LABORATORIES THE UNIVERSITY OF MICHIGAN



LANDSAT BATHYMETRY MAP
Great Bahama Bank
September 6, 1975

Color	Band 4 Digital Count	Depth in Meters
Purple	0-50	17.7-∞
DK. Blue	51-66	14.0-17.7
LT. Blue	67-88	12.0-14.0
Green	89-78	9.8-12.0
Yellow	71-68	7.0-9.8
Red	66-286	4.3-7.0
White	287-511	0.0-4.3 and clouds

FIGURE 10. BATHYMETRY MAP MADE FROM BAND 4. Site is the northern edge of the Great Bahama Bank. Clouds or shallow depths less than 4 m are white. Other depths are coded according to legend.

values for a given depth range are given in the caption for Figure 10. Fortunately, the sky was clear at station F-1 within this scene and the satellite sensor signals corresponding to the pixel containing the two ships could be identified from the CCT. This was accomplished by first rotating and scaling the Landsat data and then developing a regression equation that converts line and point numbers from the digital format into known geographic coordinates. A twelve-point fit using the geographical coordinates of distinct land features in the scene were used to compute the regression relations. Since the satellite fixes made by the Beayondan gave accurate position information, these were used to find the corresponding Landsat line and point numbers. The Beayondan's calculation for the position of station F-1 was $25^{\circ} 45.116'$ N latitude and $78^{\circ} 9.001'$ W longitude. The corresponding line and point position in the Landsat data was computed as 1524, 496 respectively. The digital count for this pixel was found to be 66. By careful examination of the digital data it was possible to locate which of the six detectors to use in determining the corresponding deep water signal in an area north of the Great Bahama Bank. This value was found to be 59 counts. Using the model described in the previous section, the relationship for station F-1 was:

$$Z = \frac{-1}{0.117} \ln \left(\frac{V - V_S}{70.4} \right)$$

where $\alpha = 0.058 \text{ m}^{-1}$ was obtained from Table 2.

$V_0 = 70.4$ for the parameters following:

$T_1 = T_2 = 0.98$

$E_0 = 12.8 \text{ mw cm}^{-2}$ (Sea Cell reading at the surface)

$T = 0.8$ (Guttman-Kwajalein atmosphere)

$r_b = 0.26$ (Derived from the underwater photography)

$k_S = \frac{127 \text{ counts}}{0.83 \text{ mw cm}^{-2} \text{ sr}^{-1}}$ (NASA-supplied sensitivity constant).

The high-gain Band 4 Landsat data for this date saturated at 127 counts. Substitution into the equation for Z gives:

$$Z = \frac{-1}{0.117} \ln \left(\frac{66-59}{70.4} \right) = 19.7 \text{ m.}$$

This is the calculated depth from the assumed model, based on careful analysis of the Landsat digital values.

On board the Calypso, the displacement of the fathometer recording pen for this site was 42.1 mm with a scale sensitivity of 10 ms/20 mm. The temperature of the water at this site was 29.1°C. Using the temperature correction of 2.4 m/s/C° above 25°C the velocity of sound was computed to be 1542 m/s.

The fathometer displacement represents a two-way path for the time it takes the sound to reflect from the bottom back to the transducer. Thus,

$$Z_f = 1542 \text{ m/s} \times \frac{t}{2} = 1542 \text{ m/s} \times \frac{42.1 \text{ mm} \times 10^{-3} \text{ sec}}{2 \times 20 \text{ mm}} = 16.2 \text{ m.}$$

The Calypso fathometer transducer is 2.97 m below the water line; this bias must be added to the value computed for Z_f . Thus, the depth Z_C measured by the Calypso for station F-1 was:

$$Z_C = 16.2 \text{ m} + 2.97 \text{ m} = 19.2 \text{ m}$$

The close agreement (2.5% error) between the 19.7 m derived from the model and 19.2 m measured by the fathometer gives strong evidence to the correctness of the approach and to the potential practical utilization of satellite data for water depth measurements.

4.3 EXTENSION OF THE CALCULATIONS TO OTHER AREAS

In order for the satellite technique to be considered practical, we must know how well other depths calculated from the satellite MSS digital values will compare with ship-measured depths. This necessarily raises the question of the reliability of the extension of measured values for α and r_b at one site to other nearby areas. This element was tested using the ship transect described in Figure 3.

Along the track, the Calypso position was known from LORAN-C measurements and the depth was known for each corresponding minute of data samples. A number of positions along this track was selected and by similar procedures to that for station F-1 the depths were calculated. In addition, the mean deep water signal in Band 4 was calculated for all six detectors separately and together. These are listed in Table 3.

One can see that the Landsat detectors are not equally noisy so that depth accuracy can vary from point to point in a scene. For this analysis, the standard deviation of 1.77 calculated for all six detectors was chosen to define the error bars on the depth calculations from the satellite data. A graph showing the calculated values versus the ship measured depths is given in Figure 11.

The ideal case would be for all values to fall on the straight line. It can be seen that agreement to 22 m depths is readily acceptable but beyond this range the calculated values are consistently lower than measured values. It is encouraging to note that for this site, depths at 40 m were detectable (even though they were not correctly measured as such). There could be several reasons for the short estimate.

First, the model has neglected scattering effects. At longer water path lengths, this assumption could be invalid. Second at deeper depths, less bottom vegetation may occur, so that the effective reflection could be higher and thus appear to be a signal from a shallower depth. In any event, the signal from the 40 m depth represents

TABLE 3

AVERAGE MSS4 SIGNALS OBSERVED
OVER DEEP WATER,
SEPT. 6, 1975

<u>Detector</u>	<u>Mean Signal</u>	<u>Std. Deviation</u>
1	57.80	1.43
2	57.34	2.05
3	57.85	1.99
4	58.68	1.55
5	57.70	1.79
6	59.09	1.05
all	58.14	1.77

Based on sample of 2100 Points for
each detector.

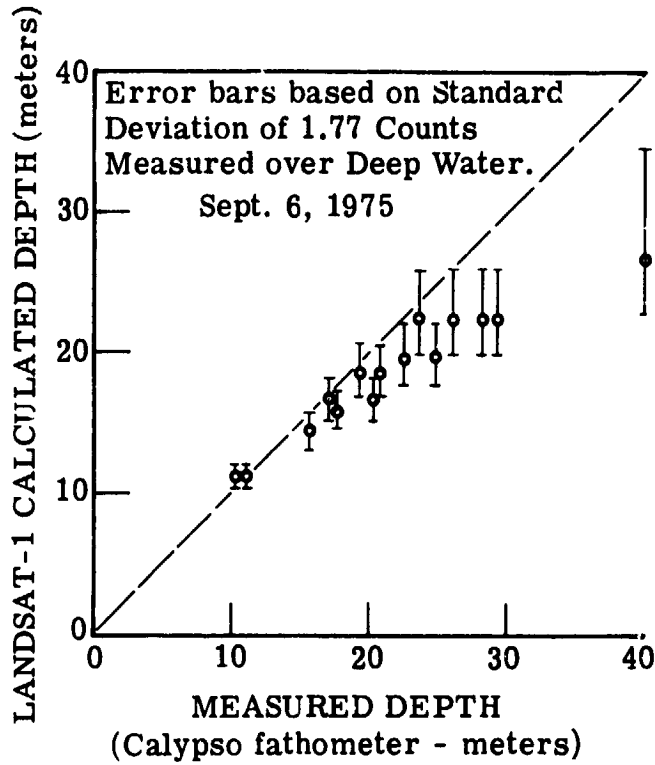


FIGURE 11.

LANDSAT-1 CALCULATED DEPTH
vs MEASURED DEPTH

only two counts above the deep water signal, indicating that the effect may also be statistical. Note the location of the upper error bar on the 40 m test case. It is close to 35 m. An error of 5 m out of 40 m is 13%. The agreement is better for shallower depths where the signal-to-noise count is more favorable.

4.4 EXTENSION OF THE CALCULATIONS TO ANOTHER DATE

A stronger test of the method can be made by assuming that the ground data taken in September is stationary in time and using it to calculate depths with Landsat CCT's obtained in October. On October 12, 1975, Landsat-1 obtained coverage of the station F-1 area. Since the solar zenith angle was different, the signal levels were found to be lower. However, the noise variation as seen in the calculation for the standard deviation in Table 4 were similar to the September case. For October, the mean signal had dropped to 51.1 counts and the standard deviation was 1.63 counts. The signal change was proportional to the $\cos \theta$ where θ is the solar zenith angle.

In a similar fashion as above, a graph comparing Landsat calculated depths versus measured depths was constructed (see Figure 12). The water transparency value and the bottom reflection value used in the model were those measured in September.

The October satellite-calculated depths followed a similar pattern. Good agreement in the 20 to 23 m range with the error on the short side for the deeper depths. Interestingly, the upper error bar for this date for the 40 m data point now crosses the correlation line.

If the signal-to-noise of the Landsat signal could be improved even by two counts better reliability would be achieved for calculated measurements to 40 m.

The results shown in Figures 11 and 12 suggest that remote bathymetry from space is practical. If the measurements of water clarity and bottom reflectance at a small number of control points can

TABLE 4

AVERAGE MSS-4 SIGNALS OVER DEEP WATER
OCT 12, 1975 LANDSAT -1

<u>Detector</u>	<u>Mean Signal</u>	<u>Std. Deviation</u>
1	51.11	1.21
2	51.45	1.57
3	51.08	1.49
4	50.52	1.93
5	51.19	1.36
6	51.60	1.89
all	51.15	1.63

Based on sample of 2100 points for each detector.

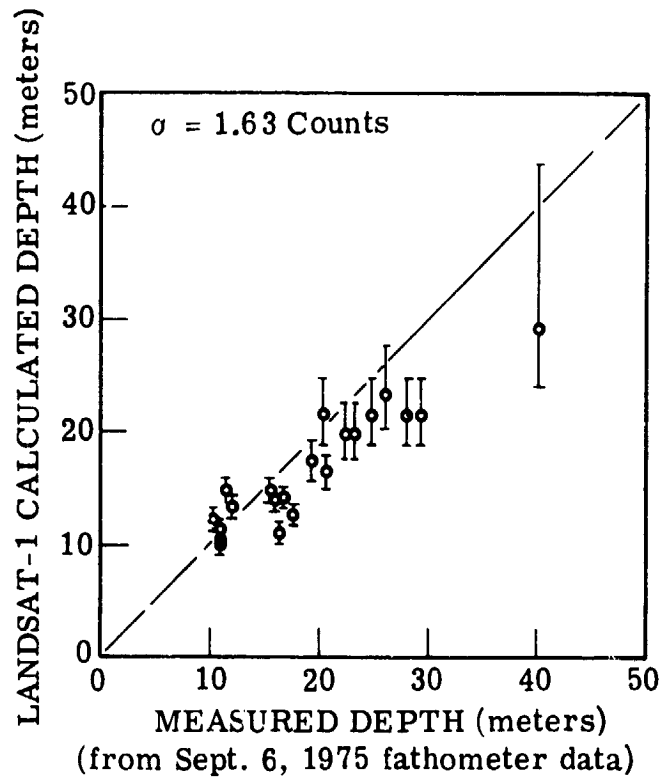


FIGURE 12
 LANDSAT-1 CALCULATED DEPTH
 BASED ON OCTOBER 12, 1975 DATA

be made and if they represent values that can be used over a few months in time, then updated charts for the location of water depths hazardous to ships is feasible. And not only can position information be derived from space data, but estimated depths with accuracies on the order of 10% or less in the range from 0 to 22 m is feasible with present satellites in orbit operating in the high gain mode. Suitable supporting data is necessary for highest accuracy and can take several forms. Knowledge of the depths at selected points can serve the same role as knowledge of water clarity and bottom reflectance. However, there is a world wide distribution of measurements from different countries of water transparency and bottom reflectance data that could be obtained and these values tested for determination of overall accuracy. One advantage of the 70 m resolution of the Landsat sensor is that small variations in the bottom surface are averaged out. With a library of parameters for different areas and with careful analysis of repetitive satellite data, charts of ocean areas with potential hazards can be constructed.

To illustrate what is possible in map construction, a relatively cloud free area of the October 12, 1975 scene for the area west of the Berry Islands was used to make a depth map. The computer output of the CCT was first rotated and scaled in order to produce a final product with proper aspect at 1:300,000. The scale was chosen to match chart N.O. 26320 covering the Northwest and Northeast Providence channels. The area on this map of the investigation is labeled Northwest channel with a reference to a very intricate passage due to hazardous shoals. The first edition of the chart is given as June 7, 1965 and it was revised February 12, 1973. A transparency of this map for the area selected from the Landsat CCT was used as an overlay to the color coded depth map generated by ERIM using the color ink-jet printer on the output of the MIDAS computer. MIDAS is a multivariate interactive digital analysis system in developmental stages under NASA sponsorship.

The map made from Band 4 is illustrated in Figure 13. The color association for each range of depth is given in the legend. The numbers on the overlay express the depth in fathoms (6 ft or 1.83 m).

The effect of noise fluctuations in the data can be seen by the texture of the dark blue area representing deep water. This is related to the differences in the mean signal levels and their variances for the six detectors as shown in Table 4.

The spurious shallow depths seen in deep water areas in the lower right are the result of the presence of clouds, cloud shadows and sun-light reflection from clouds onto the ocean surface. Obviously these artifacts can be eliminated by choosing only cloud free scenes or cloud free areas within a given scene. The general agreement between the overlay and the satellite map is encouraging. For example the pink yellow boundary which represents about 5 m depths falls on the chart between 2 to 2.5 fathoms or near 3.7 to 4.5 m.

One method to reduce the effect of the difference in signals from the six detectors operating in one band is to average their values line by line by a six by six "moving window" algorithm operating on the CCT data. This procedure was implemented and the results are shown in Figure 14. The procedure smooths the data so that each color's depth range is less ambiguous. The trade off in producing this type of map is that the spatial resolution is made coarser. The position uncertainty has been increased. However, position information can be obtained before the smoothing process.

Another benefit for depth charting is that with a 6 x 6 element smoothed data set, a single digital value can be printed which will represent a narrow depth range and produce a contour line depth profile map as shown in Figure 15.

Each line represents the depth boundary between adjacent depth ranges of Figure 14. Where the line widens that area would be interpreted as having the same water depth. Other forms of CCT processing

ORIGINAL PAGE IS
OF POOR QUALITY



FORMERLY WILLOW RUN LABORATORIES, THE UNIVERSITY OF MICHIGAN

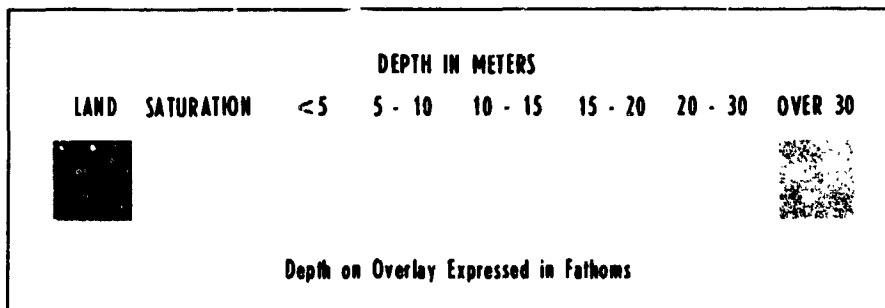
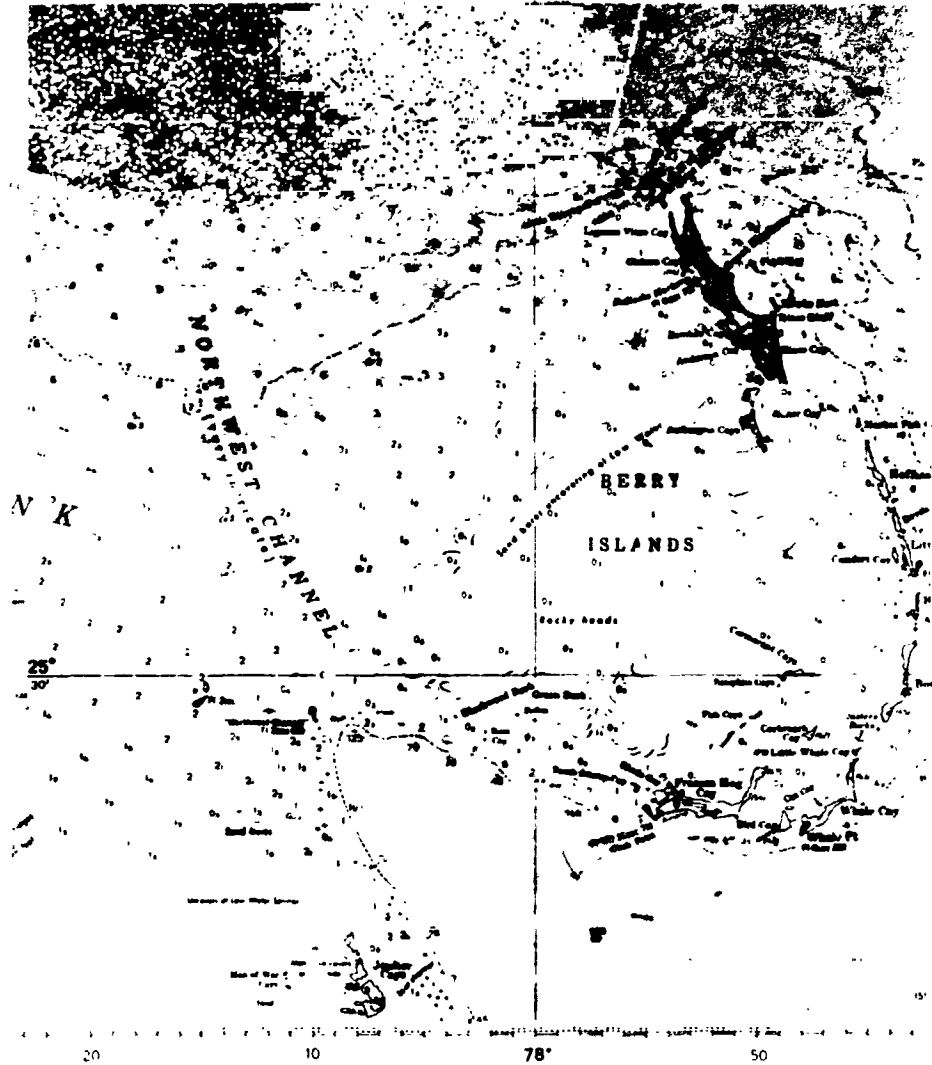


FIGURE 13. BATHYMETRY MAP FROM LANDSAT-1, BAND 4, OCTOBER 12, 1975.
With overlay from Chart N.O. 26320.

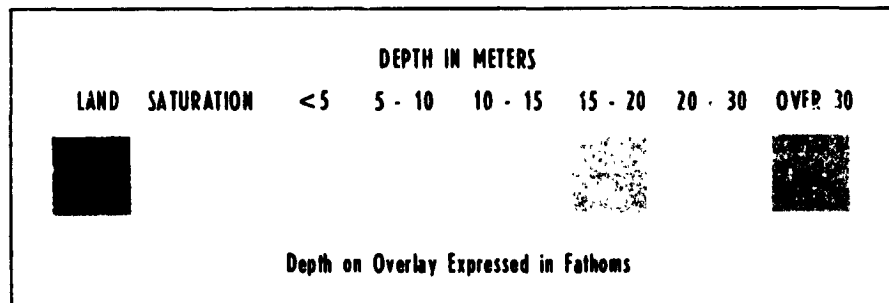
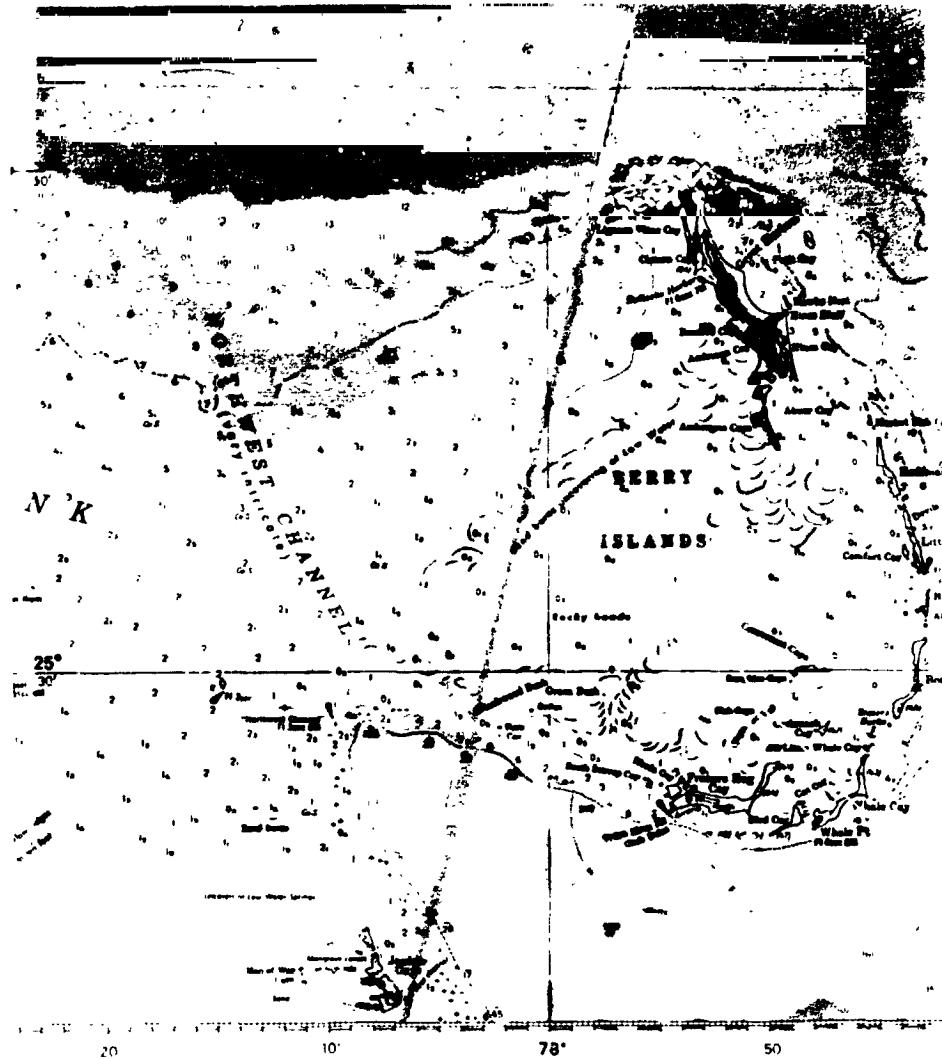


FIGURE 14. BATHYMETRY MAP FROM LANDSAT-1, BAND 4, OCTOBER 12, 1975. With overlay from Chart N.O. 26230; Data averaged over 6X6 resolution elements.

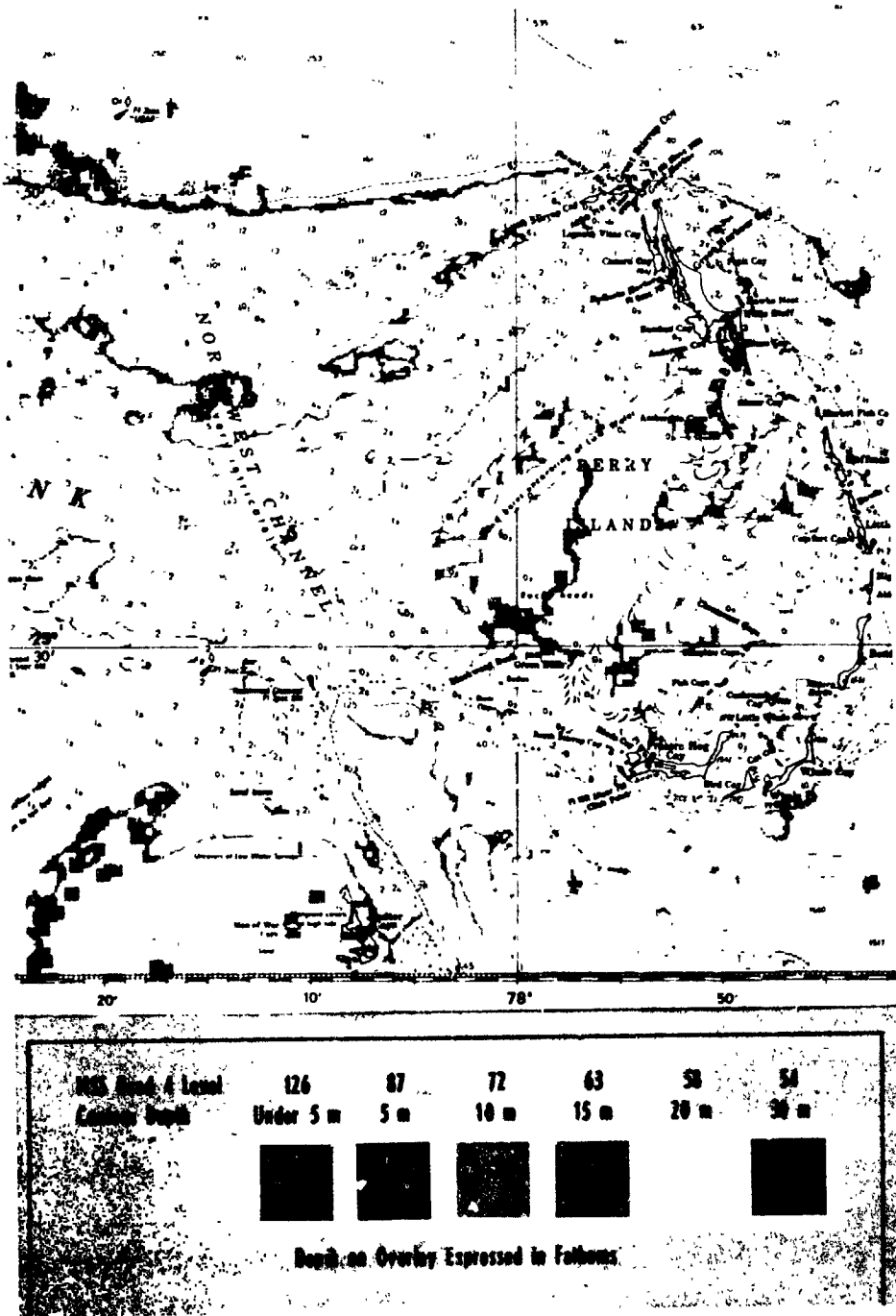


FIGURE 15. BATHYMETRY MAP FROM LANDSAT-1, BAND 4, OCTOBER 12, 1975. With overlay from Chart N.O. 26320; data averaged over 6X6 resolution elements.

are possible using the satellite data and further research could produce those output formats most helpful to the map using community.

4.5 SATURATION OF BANDS 4 AND 5

As seen from Figures 13 and 14, the red areas represent depths not measured because of signal saturation. With the high gain mode for Landsat, there will be an increase in the areas where signal saturation will occur in Band 4. This occurs in shallow depth areas, with high reflective bottom materials on the order of 30% or higher.

This aspect was further investigated for an area just north of Andros Island. Bright calcareous sands almost awash produce signal levels at 127 counts. A plot of the signal level difference versus water depth is given in Figure 16 for both Landsat Bands 4 and 5. The signal level associated with deep water for each band was subtracted from the Landsat signal to give the linear relation shown on a semilog graph. For this case depths were estimated from the chart but the error bars are calculated from the deep water noise fluctuations as before.

The data shows that for this area with the conditions prevailing, Band 4 saturates at 1.3 m while Band 5 saturates at 0.3 m. Figure 16 also explains why two channel processing for mapping depths with present Landsat MSS is limited. The minimum and maximum depths where both channels have usable data are from between 1.3 m and 6 m. This could be improved in the future by two channels operating in the blue-green and green bands of the spectrum.

The use of Band 5 (also 6 and 7, if needed) to isolate water depth at small intervals can be seen from Figure 17. There the amount of area (red color) giving a saturated signal is greatly reduced. The finer depth increments show the complimentary nature of Band 5 with regard to the range where Band 4 saturates. The higher absorption of radiation in Band 5 helps to improve the depth division with steps fraction of meters apart. In surface water hydrology or shallow-water large-transport

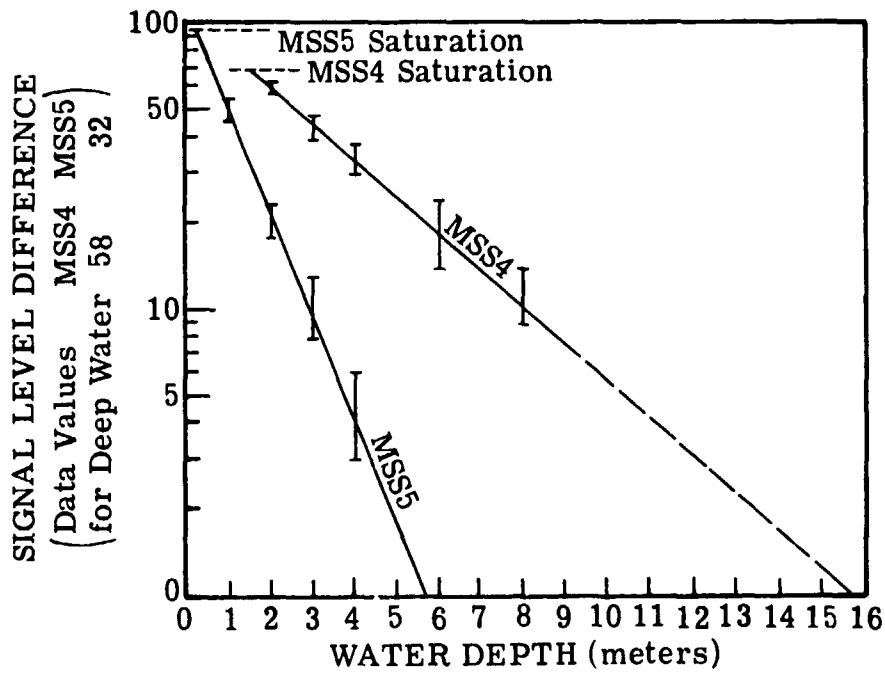


FIGURE 16. SATURATION DEPTHS FOR LANDSAT-1 BANDS 4 AND 5

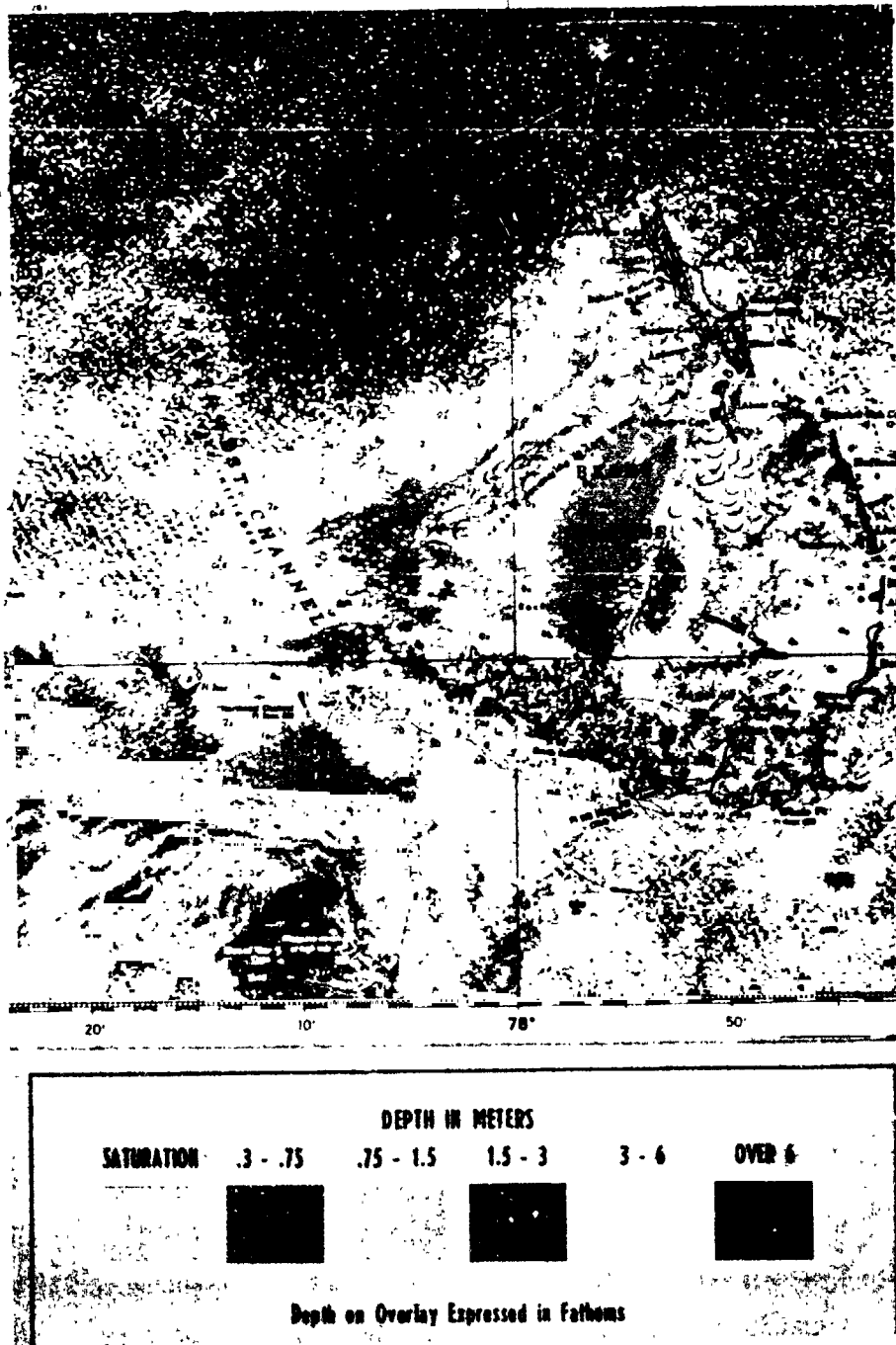


FIGURE 17. BATHYMETRY MAP FROM LANDSAT-1, BAND 5, OCTOBER 12, 1975.
With overlay from Chart N.O. 26320.

problems, such narrow level mapping of depths should prove advantageous. In a similar manner, Band 6 could be used to "slice" the shallow depth ranges where Band 5 saturates.

One notable improvement in shallow water mapping with Band 5 is that a clear passage of 3.6 m depth is shown for the Northwest channel (lower middle of Figure 17). In Figure 13, for the same area, a red zone defining a range of 0 to 5 m leaves a clear passage ambiguous.

DEPTH CALCULATIONS NEAR THE FLORIDA COASTLINE

We have seen the results for remote bathymetry from satellite data for a test area with clear water characteristics, that is, when the water extinction coefficient was equal to 0.058 m^{-1} . On the fourth day of the experiment (August 30, 1975) the Calypso anchored near the coast of Florida and obtained data at station D-1, to determine the loss of light penetration in areas of different clarity (see Table 2).

The satellite CCT data for this date was not available but the site was imaged on September 7, 1975 under partially cloudy conditions.

A portion of the east coast of Florida, extending approximately from Lake Worth to Biscayne Bay, is contained within Landsat frame 5141-14503 (September 7, 1975). A subset of this data, covering the shoreline from Port Everglades to Miami Beach, was rotated and scaled in order to yield a geometrically correct display on the MIDAS ink-jet printer at a scale of 1:80,000. The scale of the transformed data set was verified by means of an analysis of four ground control points, and the following relationships were established for the line and point numbers on the rotated data:

$$\text{line no.} = 1871 - 28.06 \times \text{lat}$$

$$\text{line point} = 280 - 23.88 \times \text{long}$$

where lat is the latitude in minutes north of 25°N , and long is the longitude in minutes west of 80°W .

The Beayondan position information from the satellite interrogations gave the coordinates for D-1 at $26^{\circ} 3.8556'\text{N}$ and $80^{\circ} 5.648'\text{W}$. Using the above relationships, the line and point numbers for Station D-1 were determined to be 79 and 145, respectively. A display of the data from the CCT showed the signal values at this location to be 68 counts in MSS 4 and 34 counts in MSS 5.

An area of deep water further offshore was found to have a mean signal of 61.82 counts with a standard deviation of 2.99 counts in MSS 4, and a mean signal in MSS 5 of 34.61 counts with a standard deviation of 2.64 counts.

The signal variation in the deep water area for this data was found to be higher than that found near the Berry Islands. We interpret this to mean that the water color (and hence the returned signal to the sensor) near Florida is considerably more variable spatially because of the presence of the Gulf Stream, river discharges and ocean outfalls, and other industrial effluents along the Florida coastline which contribute to the variation in light scattering and absorption.

The signal level of 68 counts for station D-1 against a mean deep water signal of 61.8 counts clearly indicates that a bottom reflected component exists in MSS Band 4. This is not true for Band 5, where 34 counts at station D-1 is less than 34.6 counts for the deep water signal.

In order to calculate the depth at station D-1 the various ground measurements, including the underwater photography of the gray scale against the bottom, were analyzed to yield a bottom reflectance of 20%; the photometer data gave an extinction coefficient of 0.1067 m^{-1} in MSS 4 at this location. As a practical matter, the film negatives with the gray scale are scanned with a densitometer and the film density (or transmission) is plotted versus the known panel reflectance. An average film density (or transmission) was measured for the bottom and the bottom reflectance is obtained. However, this quantity measured from data taken under water can be defined as the wet reflectance = $\frac{r_b}{n^2}$ where r_b was defined as bottom reflectance in Section 4 and n is the index of refraction. When we report $r_b = 20\%$ for D-1 or $r_b = 26\%$ for F-1 these values are the dry reflectances. Substituting the appropriate values in the depth equation (see Section 4) gives the following relationship between water depth and MSS 4 signal:

$V_0 = 54$ for this site since the r_b is different from that of site F-1

$$V = 62 + 54 e^{-0.2134z}$$

$$\text{or } z = \frac{0.1}{0.2134} \ln \frac{V-62}{54}$$

This equation yields a depth of 10.2 m at Station D-1.

The fathometer reading for this site on August 30 gave a depth value of 11.2 m following the procedure described for site F-1. Again the agreement is encouraging. The higher extinction coefficient, however, limits the maximum depth measurable at site D-1. In order to determine the range of depth detectable along the Florida shoreline, two transects perpendicular to shore were investigated. One transect covered the track of the Calypso for this site and is shown in Figure 18a. The second transect was taken near Sunny Isles (25° 59.75'N) and corresponded to a fathometer line measured two years earlier by ERIM personnel in the same test area. This is shown in Figure 18b. The plot shows CCT count versus point number or position offshore. The CCT data was averaged in rectangular arrays 5 x 1 pixels with the long axis parallel to the coastline. The fairly smooth curves can be used to investigate the maximum depth penetration under these more difficult circumstances. Figure 19a and b show the conversion to depths using the equation given above.

For the Sunny Isles transect, a plot of the ground truth is also shown for comparison. Good agreement is found to depths of 8 m within the first 1,000 m from shore. Subsequent points further from shore were calculated to be deeper than measured depths. This implies a change (lower) in the value for the bottom reflection. A corrected value would have to be inserted into the model for this part of the transect. Beyond 2,200 m from shore, where actual depths are greater than 14 m, the satellite depths are shallower than measured values, producing the effect noted for clear water beyond a depth of 22 m (see Chapter 4).

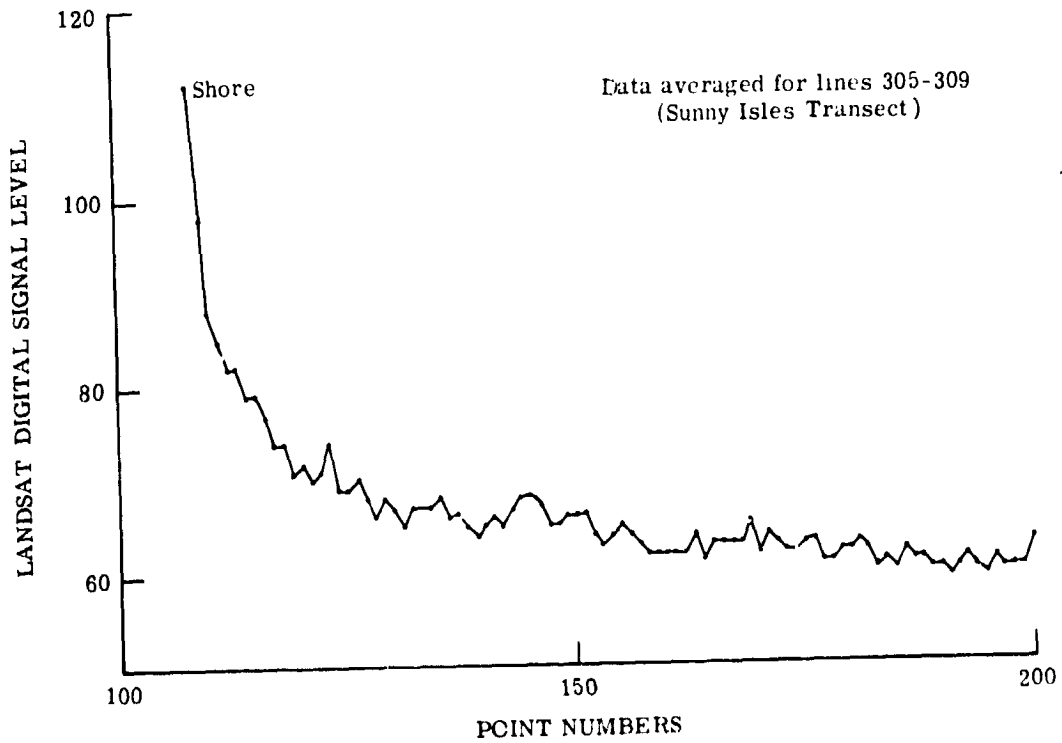
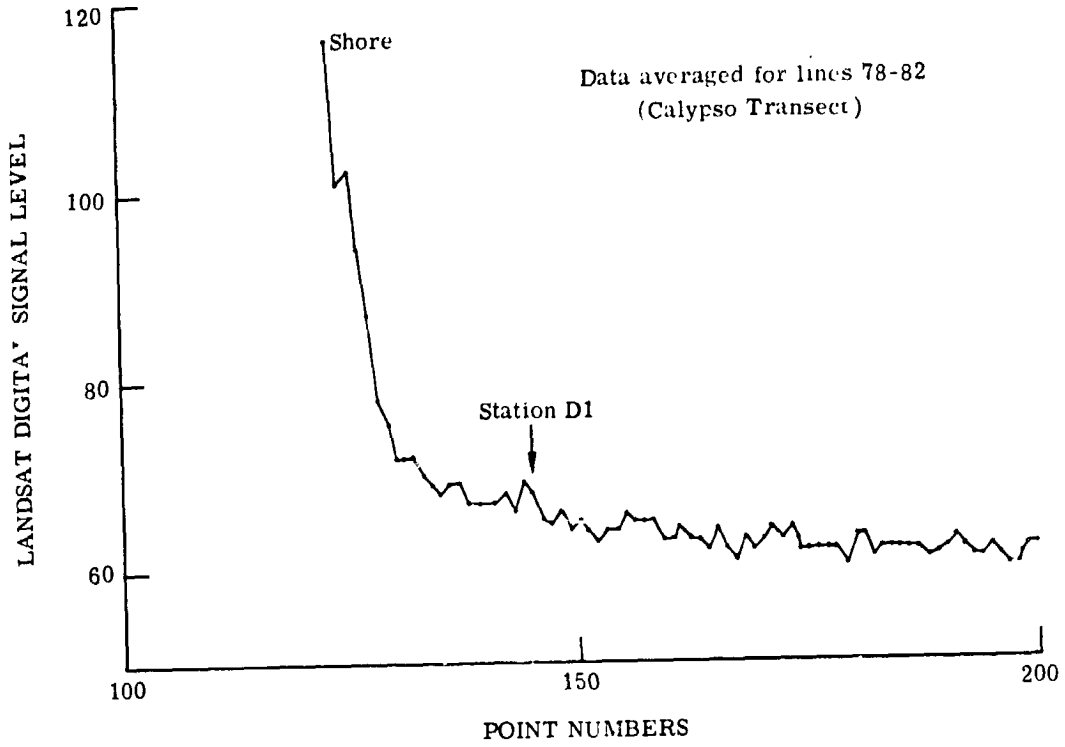


FIGURE 18. SIGNAL-RELATED DEPTH PROFILE NEAR FLORIDA CCASTLINE

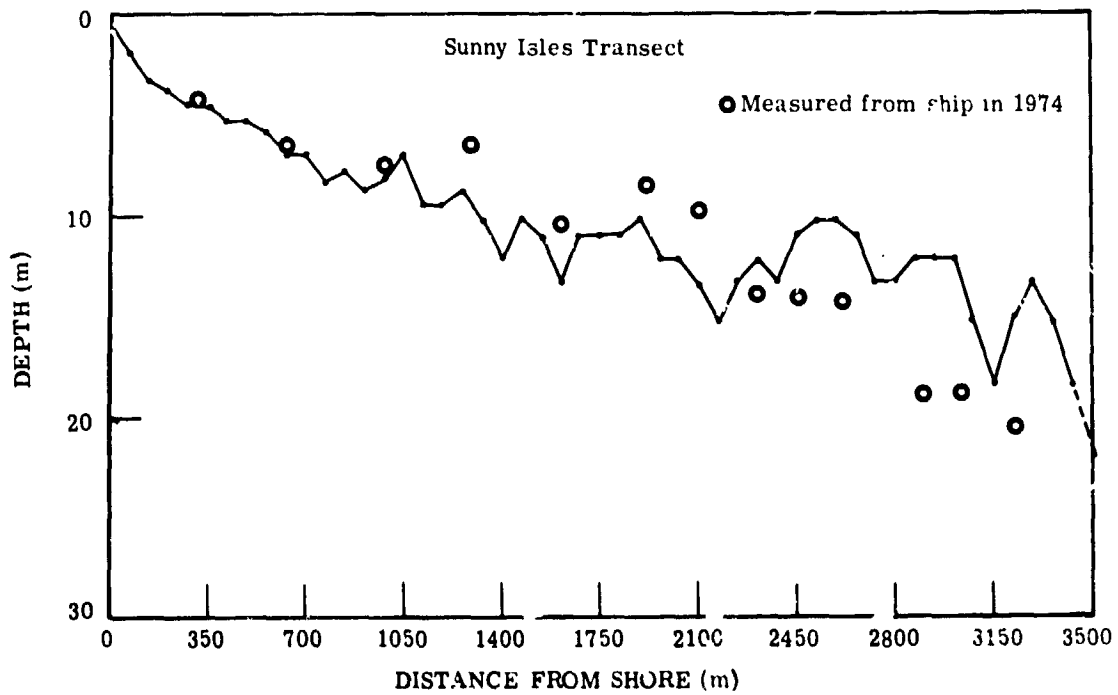
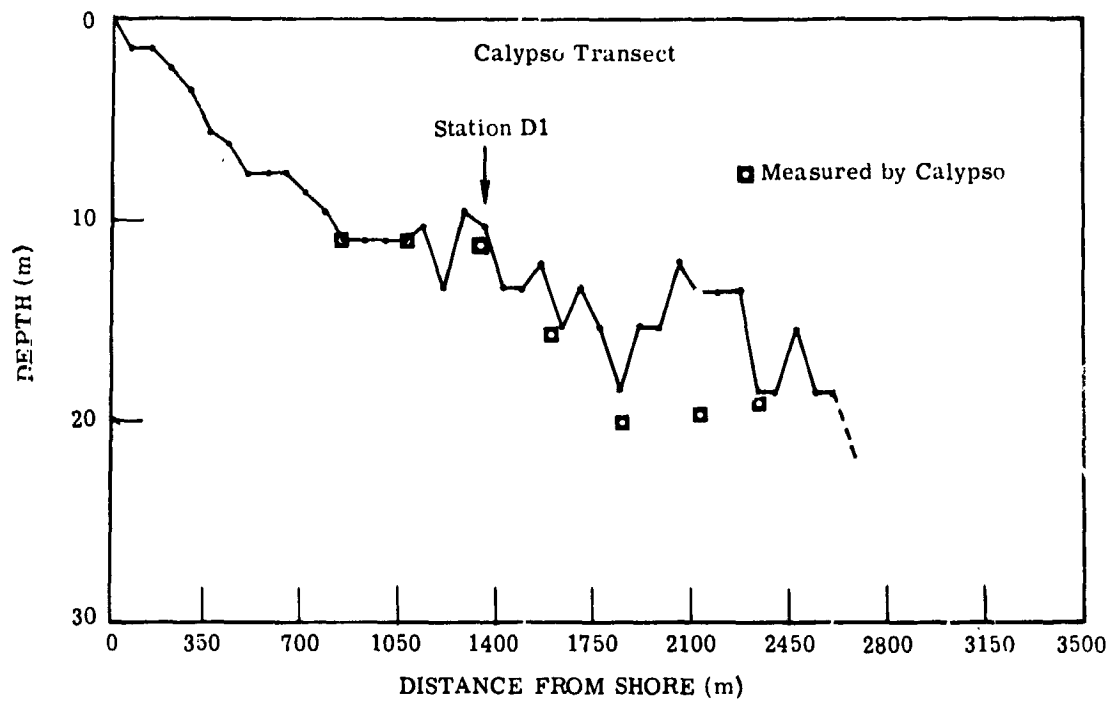


FIGURE 19. SATELLITE CALCULATED DEPTH PROFILES FOR TWO TRANSECTS NEAR HOLLYWOOD, FLORIDA

A color coded depth chart for this site was also produced on the MIDAS Ink-jet printer (see Figure 20). Depths from 0 to 15 m are indicated in 3 m increments by means of six colors on this chart. These colors and the corresponding data and depth ranges are indicated in Table 5. Land is indicated by overprinting in black those areas where the signal in MSS 7 is greater than 12 counts. A few pixels are also visible with a pink color: these indicate pixels where the MSS 4 signal was saturated in high gain mode. The data presented in this display were smoothed 5 lines by 1 point in order to reduce random noise while maintaining spatial resolution in the perpendicular-to-shore direction.

A cloud present in the image near shore gives the anomalous shallow water reading. The scale of 1:80,000 was matched to chart C&GS 11466 from which the overlay to the color coded map was made.

Numbers of the chart are expressed in feet. The correspondence of the location of underwater variations along shore in the chart to that of the satellite map is favorable. The feasibility of the technique is again demonstrated even though only shallow depths are measurable because of the higher extinction coefficient. The maximum depth discernable along the track containing station D-1 is about 18.5m.

TABLE 5

COLOR CODE FOR DEPTH RANGE
OF FLORIDA COASTLINE MAP

DATA RANGE	DEPTH RANGE (meters)	COLOR
1- 64	> 15	Purple
65- 66	12-15	Light Blue
67- 70	9-12	Green
71- 77	6- 9	Tan
78- 90	3- 6	Yellow
91-126	0- 3	Red
Saturation		Pink
	Land	Black

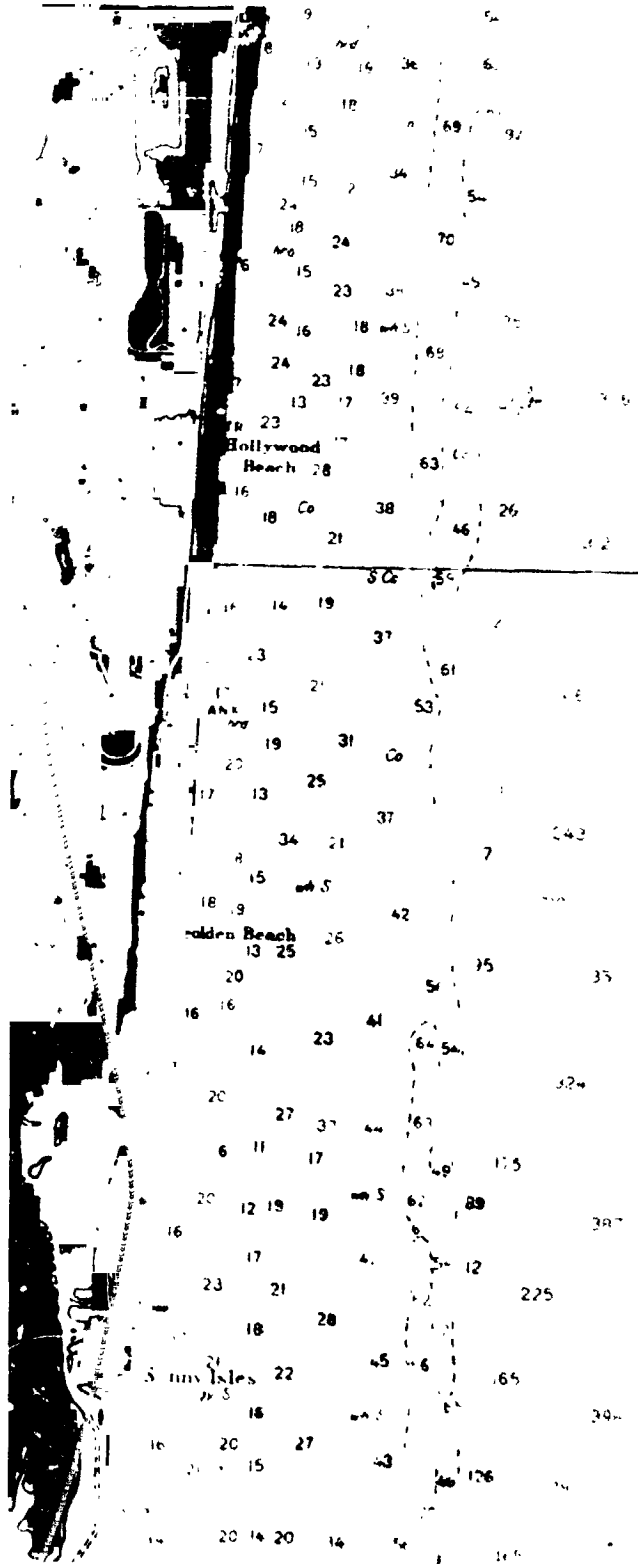


FIGURE 20.

COLOR CODED DEPTH MAP
MADE FROM LANDSAT IMAGE.
Taken September 7, 1975.
Overlay is from Chart
C&GS 11466 at approxi-
mately 1:80,000; sound-
ings are in feet. The
anomalies offshore are
due to clouds.

CONCLUSIONS

The success of the satellite calculated water depth using high gain Landsat MSS 4 data demonstrated the feasibility of remote bathymetry from space. In clear water (extinction coefficient = 0.058m^{-1}) depths to 22 m can be measured reliably and signals from 40 m depths can be differentiated sometimes from deep water signals that are due to scattering only. In less clear water (extinction coefficient = $.11\text{m}^{-1}$) depths to 10 m are reliably measured and detection of the presence of 18.5 m depth is feasible. For these values to be generally realizable, the bottom reflection should characteristically be between 20 to 26% in the green band (Landsat MSS 4). The best accuracy of the depth measurement will occur if knowledge of the areas average water transmission characteristics are known as well as the reflectance of the bottom.

Single-channel charting is reliable where assumption of uniform bottom reflection and water transmission characteristics are valid. If changes do occur, adjustments of the appropriate model input parameters must be made to maintain accuracy. Otherwise those pixels should be edited. The technique may use alternative information to bottom reflectance and water clarity. Knowledge of depths at control points within the scene, made available by water level gauges or by aircraft with laser depth-ranging equipment and ship support measurements are equivalent. A catalog of average values for an area will give useful a priori information. Repetitive satellite coverage helps provide information as to possible deviations from average values.

Under certain conditions of bright bottom reflectances, 30% or greater and shallow depths, less than 1.3 m, the high gain data of Band 4 will saturate. In this case, it is possible to use Band 5 data to determine depth in fractions of meter steps for the range where Band 4 saturates because of the greater light attenuation in Band 5.

Cloud free Landsat scenes offer the best solution to depth map construction to avoid anomalous shallow depths due to clouds and ocean reflection of sunlit clouds. Incorporation of scattering effects into model relating Landsat signals to water depth could improve accuracies of deep water estimates.

Detection of deeper depths or improved reliability of intermediate depth calculations would be possible if optimum band location could be employed on future spaceborne sensors. An analysis of the effect on S/N ratio by placement of the channel bandwidth between .45 to .60 μm was made on 0.1 μm intervals [3]. That study concluded that improvement in S/N would occur by placement of the band in the range .47 to .57 μm . The same methodology of that study was employed to determine placement with .07 μm bandwidth intervals. The results are shown in Figure 21. The analysis was done for three types of water clarity and two atmospheric conditions. The graph shows the improvement to be gained by proper location of the channel bandwidths. For clear water, 0.45 to 0.52 μm would be optimum. As a compromise to all three types of water, 0.47 to 0.54 μm might be selected. The NASA/Cousteau Ocean Bathymetry experiment also demonstrated the potential of near-real-time transmission of processed satellite data to ocean going vessels through ATS-3 communication link. The report of this phase of the experiment is given in Reference 5.

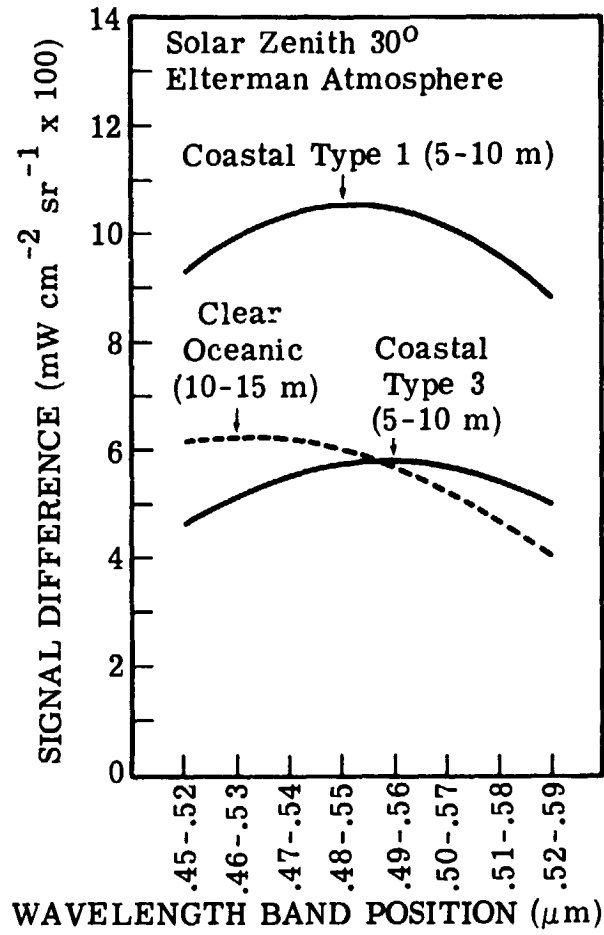


FIGURE 21. SIGNAL DIFFERENCE VERSUS BAND POSITION (LANDSAT-D)

REFERENCES

1. W. L. Brown, F. C. Polcyn, A. N. Sellman, and S. R. Stewart, Water-Depth Measurement by Wave Refraction and Multispectral Techniques, Report No. 31650-31-T, Willow Run Laboratories, Ann Arbor, August 1971.
2. F. C. Polcyn and David R. Lyzenga, Remote Bathymetry and Shoal Detection with ERTS, Report No. 193300-51-F, Environmental Research Institute of Michigan, Ann Arbor, April 1975.
3. D. R. Lyzenga, C. T. Wezernak, and F. C. Polcyn, Spectral Band Positioning for Purposes of Bathymetry and Mapping Bottom Features From Satellite Altitudes, Report No. 115302-1-F, Environmental Research Institute of Michigan, Ann Arbor, January 1976.
4. A. Guttman, Extinction Coefficient Measurements on Clear Atmospheres and Thin Cirrus Clouds, Applied Optics 7, 2377, 1968.
5. Dr. John Barker, NASA Goddard, in preparation.

APPENDIX A

Technical Memorandum S3R-76-067

ANALYSIS OF LORAN-C DATA COLLECTED ABOARD
CALYPSO DURING OCEAN BATHYMETRY EXPERIMENT

April 1976

The Johns Hopkins University
Applied Physics Laboratory

S3R-76-067
IW10S3R0
April 19, 1976

TO: Distribution

FROM: E. E. Westerfield

SUBJECT: Analysis of LORAN-C Data Collected Aboard Calypso
During Ocean Bathymetry Experiment

BACKGROUND

In July of 1975 NASA requested that APL investigate the feasibility of accurately determining the position of Jacques Cousteau's ship Calypso during a joint Cousteau Society/NASA operation. The purpose of the operation was to determine the feasibility of accurately determining depths of water in shallow areas utilizing data from the LANDSAT satellite. APL was specifically requested to look into installing a TRANSIT Navigation receiver aboard the Calypso and to work with the Coast Guard in the use of LORAN-C. Preliminary studies indicated that it would be difficult to install TRANSIT gear aboard the Calypso due to very limited space, plus an uncertain power system. This was particularly true since Backpack equipment, which is capable of battery operation, was not in any condition to be utilized at that time and time was not available to put it in condition. In addition, it appeared that Calypso would be constantly in motion and that it would be difficult to obtain a sufficient number of passes at any one point for high quality position determination.

It was suggested by Laboratory personnel that the TRANSIT gear be installed aboard another vessel that could support the gear adequately and that would accompany the Calypso. The Laboratory's 85 ft. Motor Sailboard Beayondan was picked for this job, principally because it was available and required a relatively small crew to operate.

PRECEDING PAGE BLANK NOT FILMED

The proposed method of operation was for the Beayondan to sail to one or two sites in each area and to anchor long enough to accurately survey the location by means of the Navy Navigation Satellite system (TRANSIT). The Beayondan was also equipped with LORAN-C gear so that the LORAN grid could be accurately calibrated at each point.

At NASA's request the Coast Guard installed a LORAN-C receiver aboard the Calypso. The receiver was a unit that APL had purchased for the Coast Guard and loaned back to the Coast Guard for this operation. Coast Guard personnel installed it aboard the Calypso in Nassau. This receiver was a Deca ADL81. The purpose of this receiver was to determine Calypso's position while it was underway and too far from Beayondan for Calypso's position relative to Beayondan to be accurately determined using visual means.

PURPOSE OF THIS REPORT

The purpose of this report is to serve as a vehicle to disseminate the data recovered by processing the LORAN-C data collected aboard Calypso, during four of the data collecting runs.

OVERVIEW OF LORAN SYSTEM

LORAN is a hyperbolic radio navigation system that makes use of a master and two or more slave stations. Each station transmits a short pulse of 100KC carrier at a rate of approximately 10 times per second. The exact rate varies from chain to chain. All LORAN-C stations transmit on a frequency of 100 KHz. Precise navigation cannot be obtained by using the pulses, so a system is utilized whereby measurements are made using the 100 KHz carrier. This is done by a method known as cycle matching. The third positive going zero crossing of each pulse is considered the epic point for the pulse.

The LORAN-C receiver is built in such a manner that it can track a master station and up to three slave stations at once. The receiver displays the difference in arrival time of the signal received from the master station and each of the (TD) slave stations being tracked in microseconds. The receiver used aboard Calypso was capable of tracking three slaves. One of the difficulties with the receivers and the system in general, is that it is necessary that the receiver lock on and track the third cycle as received from the master and all the slaves. When the signals are very weak the receivers tend to track the wrong cycles, resulting in an error in the time difference measurement, i.e., the difference in time between when the master station was received and a particular slave, by some multiple of 10 microseconds. This can result in a significant error in navigation.

In the area of operation the master station, which is located at Cape Fear, is received quite well, as well as the signal from Jupiter, one of the four slave stations of this chain. The signals from the slaves located at Dana, Indiana, Newfoundland and Nantucket, however are quite weak. This resulted in the receiver often tracking on the wrong cycle or switching cycles in the middle of the data run. In addition, the geometry of the LORAN-C stations as viewed from a user in the area is poor. The lines of position (lines of constant time difference) obtained between the master and the various slaves are running very near parallel. As a result, a very small error in measuring the time difference can result in a relatively large position error. This is particularly true as one approaches the coast of Florida, where one is near the baseline of the Cape Fear - Jupiter pair.

In addition, it appeared that the LORAN-C receiver aboard the Calypso was not functioning too well. The receivers are equipped with a series of lights to indicate when they are properly locked on the stations. This receiver often gave an indication of being properly locked even though it was not locked or was locked onto the wrong cycle.

DATA COLLECTION

The data was manually recorded by Calypso personnel on log sheets during the various data collection runs of Calypso. The runs were arranged so that typically Calypso ran very near, i.e., usually within 50 feet of Beayondan, at least once during the run. This proved to be invaluable in that the position of Beayondan, which had been obtained by means of the Navy navigation satellite, could be utilized to calibrate the Calypso LORAN-C receiver. This information could be used to determine which stations were being properly tracked, i.e., if the receiver was tracking on the correct cycle and if not what the correction factor was.

PROCESSING OF DATA

To obtain the best estimate of Calypso position while it was underway, was a very involved process due to the relative poor quality of the data, plus occasional errors in the hand recording process.

The data was first punched on IBM cards. The cards were then read into a Honeywell H21 computer where they were stored on disc. Use was then made of a Hewlett-Packard 9821 calculator with associated plotter. Hardware was available that allowed the data to be read directly from the disc and entered into the calculator. The first step in the processing was to plot the time

difference that had been read from the card against time. Jumps of 10 microseconds in the data could be readily seen from the plots plus other errors such as punch errors could be readily seen. The cards were corrected until a smooth curve was obtained from each set of TD's.

The TD's collected by the Calypso receiver at the time of closest approach were compared to TD's computed for the position. Routines were then utilized for offsetting the TD's normally by a multiple of 10 microseconds, to make them nearly agree with the computed TD's for the point of closest approach.

The TD's for the complete run were then smoothed by utilizing a linear regression algorithm where a straight line is fitted to each set of 7 consecutive points, in a least squares process. The equation of the line is then used to calculate the TD of the center of the line. This was repeated for each data point, always utilizing the data collected for that point and three points on each side. In the case of the end points, the value is calculated from the coefficients of the nearest 7 point segments.

Utilizing the smooth TD's, the position at each point was calculated utilizing a standard LORAN-C computational algorithm. The positions were then plotted along with the positions of both Beayondan and Calypso when at anchor. In some cases the data was still quite ragged and additional smoothing was done directly on the latitude and longitude number utilizing the same algorithms used for the TD's, i.e., where a straight line is fitted to 7 consecutive data points.

PROCESSING OF DATA

Four sets of data collected aboard Calypso have been received from Mr. Fabian Polcyn of the Environmental Research

Institute of Michigan, who was principal investigator for the experiment. This data covers the following time spans.

27 August 04:30 to 06:48 local time
27 August 10:36 to 11:23 local time
28 August 03:17 to 05:48 local time
6 Sept. 04:25 to 07:57 local time

The unique features of processing each data run is discussed below.

27 August 04:30 through 06:48

During the majority of this run personnel aboard Calypso recorded data from three slave stations. All three possible combinations were then processed, i.e., Jupiter/Nantucket; Jupiter/Newfoundland and Newfoundland/Nantucket. Following the position computation, data from each station pair was plotted. As was predictable knowing the typical strength of the signal, the Jupiter/Newfoundland data was by far the best, being very smooth and not requiring any post position computation filtering. The other data was much noisier with the Newfoundland/Nantucket data being essentially useless. This was due not only to the fact that the signals were weak, but also that the paths to both slave stations from the vessel are nearly coincident and as a result a very poor geometric solution is obtained. Data from this pair deviated by over 4 miles at times from the data of the other pair. The difference between Jupiter/Newfoundland and Jupiter/Nantucket was half a mile at the worse. The Jupiter/Newfoundland data agreed much better with the NAVSAT data. Figure 1 is a plot showing the results of computations utilizing all three pair. Figure 2 is a more detailed plot showing only the Jupiter/Newfoundland data. X's are shown at each data point. Data was typically collected every minute and the time is indicated every 10th point.

In addition, the positions of the Beayondan at six o'clock and at eight o'clock are plotted as well as the position of the Calypso before and after the data runs. The position of the Beayondan was obtained via the Navy navigation system and is accurate to around 15 meters for the 8 o'clock position and to 100 meters for the 6 o'clock position. The error of this fix is due to the fact that only one pass was taken so that no exact statistics can be arrived at. Figure 2 not only shows the current run under discussion, but also the run made between 10:26 and 11:23 local. Figure 3 shows the data for this run without the time marks. The turn at the end of the run can be seen from this plot. Table 1 is a listing of the processed data giving the best estimate of the latitude and longitude at each time point. For this run Jupiter and Newfoundland required essentially no correction at all. The run made utilizing Newfoundland required a 10 microsecond correction, i.e., the receiver was 1 cycle away from the proper third cycle of tracking.

27 August 10:34 to 11:30

Data for this run was available from three different slaves. As usual the data from the Jupiter slave was good while that from Nantucket and Newfoundland was weaker with the Newfoundland/Nantucket pair being weak enough that it was not utilized. In the case of Newfoundland the receiver was 4 cycles off, i.e., 40 microseconds. This error was detected by comparing the Calypso TD's to that collected aboard the Beayondan. The actual comparison was done when Calypso was anchored and range and bearing was taken from Beayondan to Calypso via radar and hand compass. The Beayondan position was from NAVSAT. Figure 4 is a chart showing the data and Table 2 lists the processed data. The position of Beayondan and Calypso when at anchor is again shown on the chart. The reader should note the high scale factor for this particular chart.

28 August 03:19 to 05:52

Data was again recorded from Jupiter, Nantucket and Newfoundland. Again the signal from Nantucket was obviously very weak as the receiver was often unlocked. All data processing was therefore done with the signals from Jupiter and Newfoundland. The signal however, was off by 60 microseconds, i.e., 6 cycles, which was corrected in processing. The time differences were filtered prior to the position computation. Figure 5 is a plot of the computer positions prior to the insertion of post processing filtering, while Figure 6 is a plot of the position after filtering. The position of the Beeyondan at its anchor point is also plotted. It appears that the second filtering probably improves the data because it is very unlikely that the ships made sudden changes of course as indicated by the unfiltered plot. Table 3 is a listing of the filtered positions vs time.

6 September 04:25 to 07:57

Data was collected from the three slave stations. However, for this run the Newfoundland data was very sporadic, while the Nantucket data was quite usable. Nantucket/Jupiter was therefore used for all data runs. No major corrections were required, i.e., the receiver appeared to be tracking on the proper cycle. The data was sufficiently noisy, however, that post processing filtering was utilized. Figure 7 is a chart showing movement of Calypso while Table 4 lists the position as a function of time. Tables 5 and 6 summarize the results of NAVSAT data collected aboard Beeyondan, including the bias errors noted for the LORAN-C grid. The position computed for Calypso when at anchor is also shown. This was computed using Beeyondan position and offsetting using range from either radar or optical measurement devices, and bearing obtained by hand compass.

CONCLUSION

The LORAN-C results shown here are probably accurate to around 200 meters, i.e., 1/10 of a mile. This number cannot be proven but it is based on the accuracy of closures with Beayondan typically found in processing the data. Considering the difficulty with the LORAN data, the availability of Navy navigation satellite data made it possible to process the LORAN data with reasonable accuracy. LORAN-C and TRANSIT are an excellent combination, in that the TRANSIT can give high accuracy when the ship is at anchor while LORAN-C can provide reasonable accuracy when underway. It is felt that if the operation had been carried out in an area where LORAN-C was better, then the data processing operation would have been simpler and the results would have been obtained much faster.

E. E. Westerfield
E. E. Westerfield

EEW:nt
Distribution
LFFehlner
RBKershner
RWLarson
DJMitola
TThompson
EEWesterfield
ives - 2
1. e

CALYPSO POSITIONS 27 August 04:30 thru 06:48

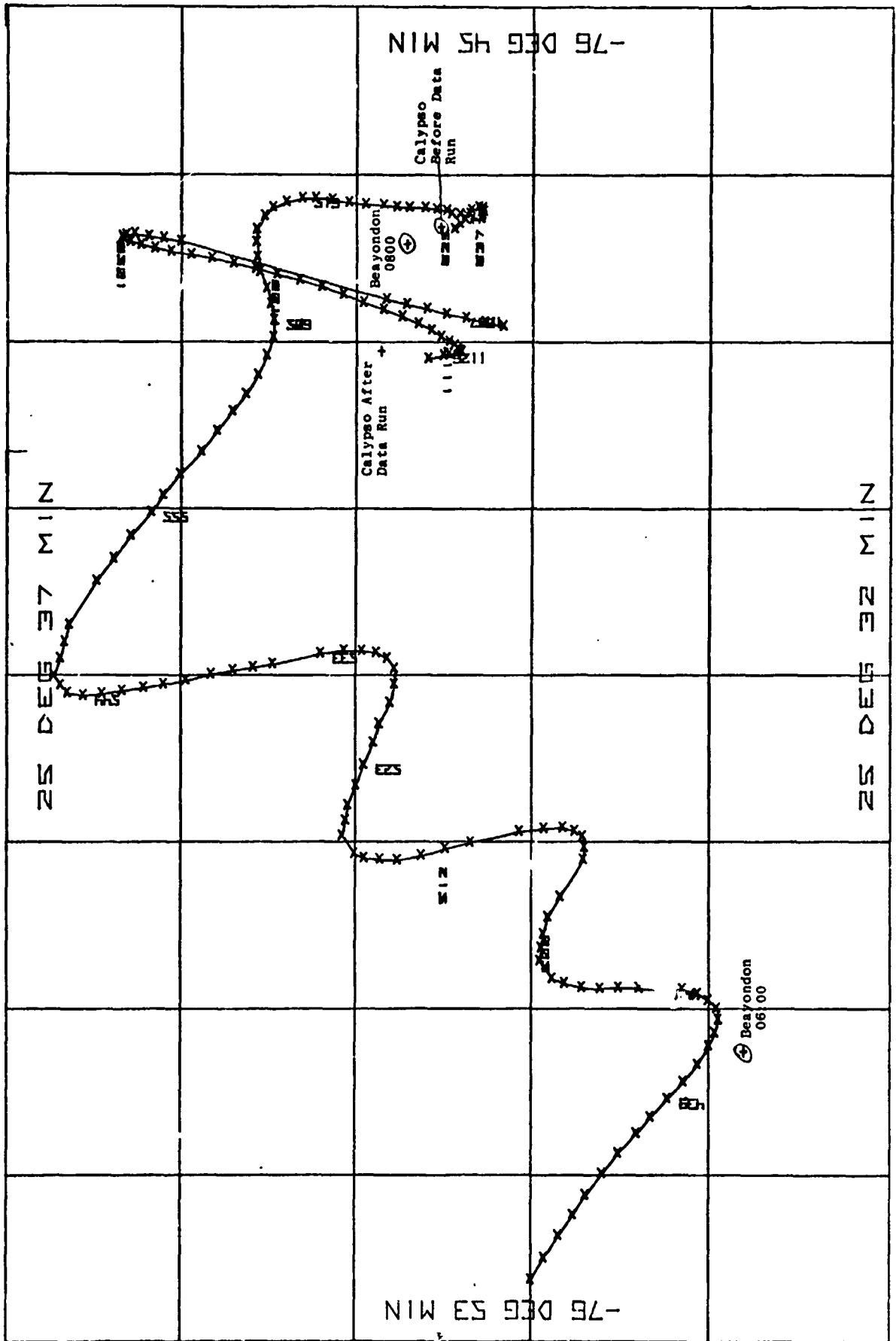


Figure 2

CALYPSO POSITION 27 August 04:30 thru 06:48

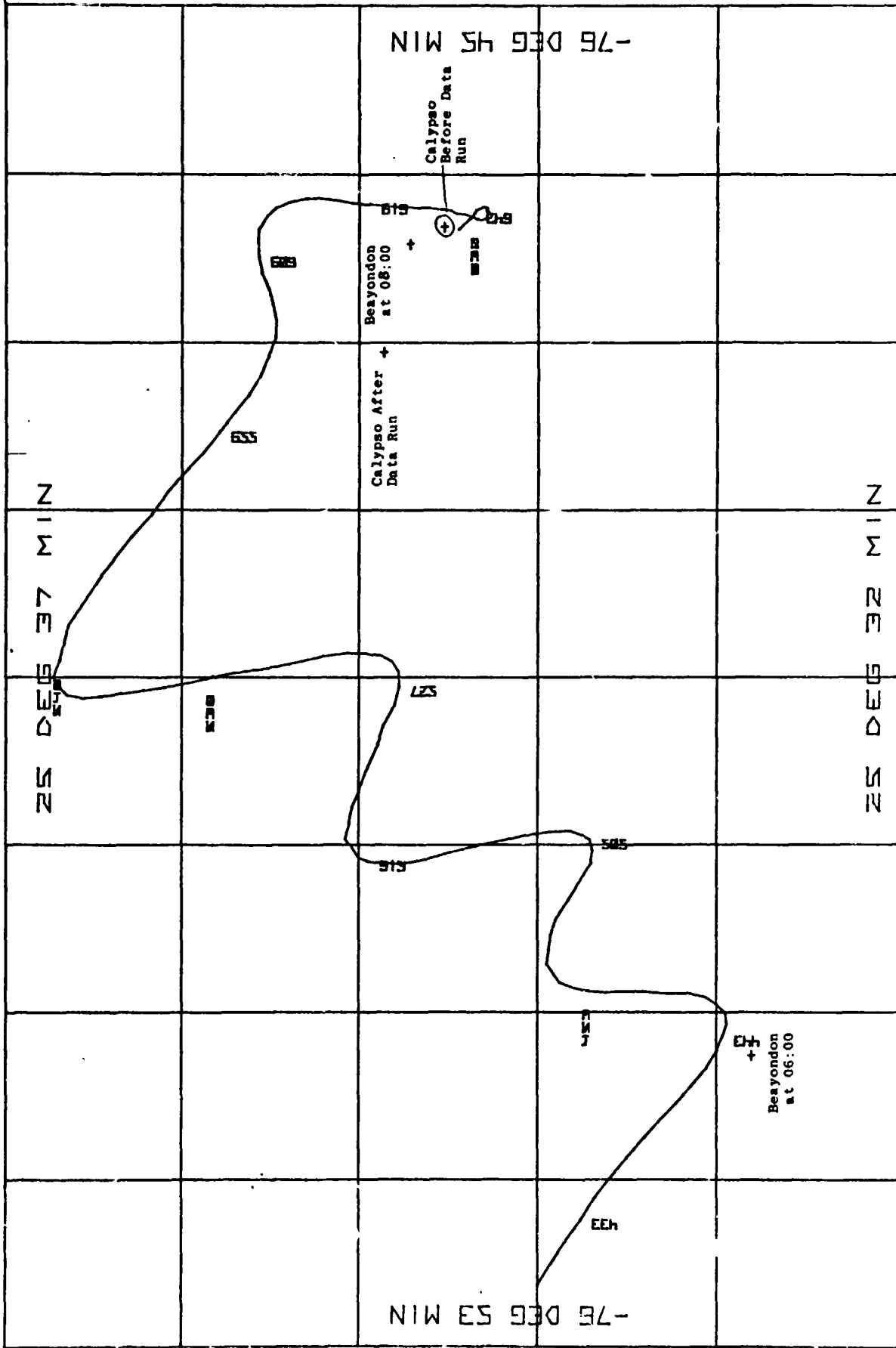


Figure 3

CALYPSO POSITION 27 August 10:36 thru 11:23

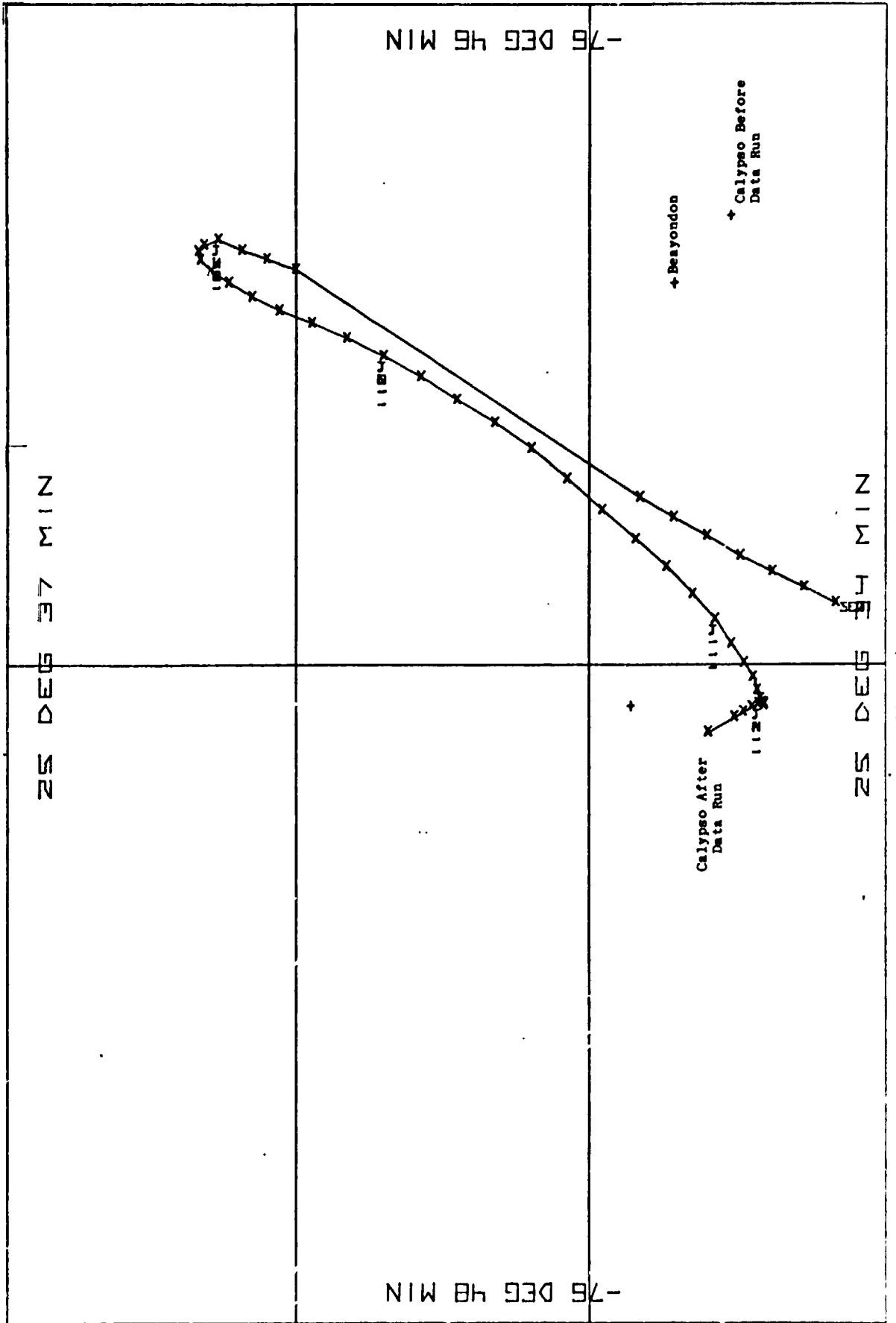


Figure 4

CALYPSO FILTERED POSITION 28 August 03:17 thru 05:48

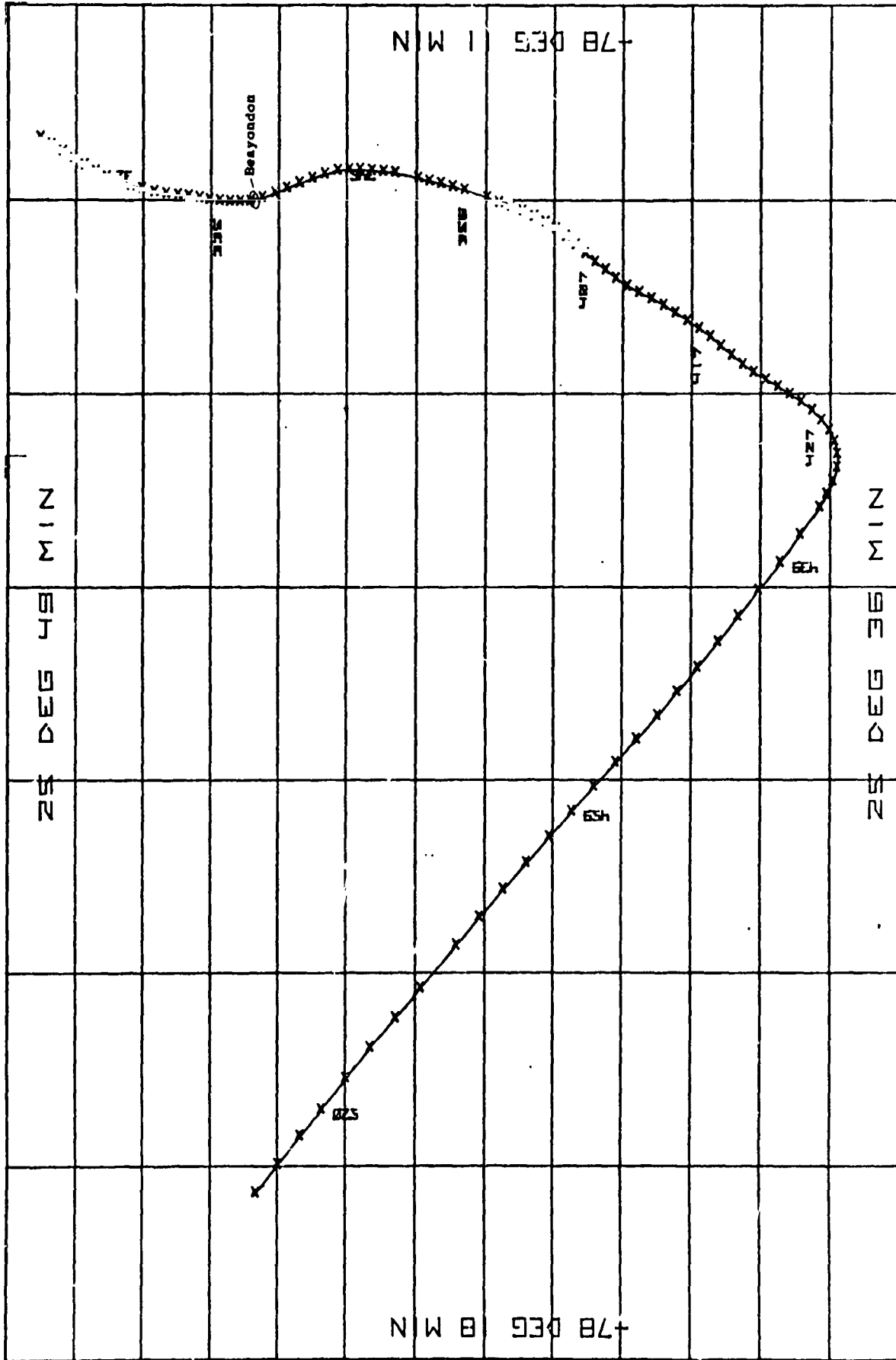


Figure 6

CALYPSO UNFILTERED POSITION 28 August 03:17 thru 05:48

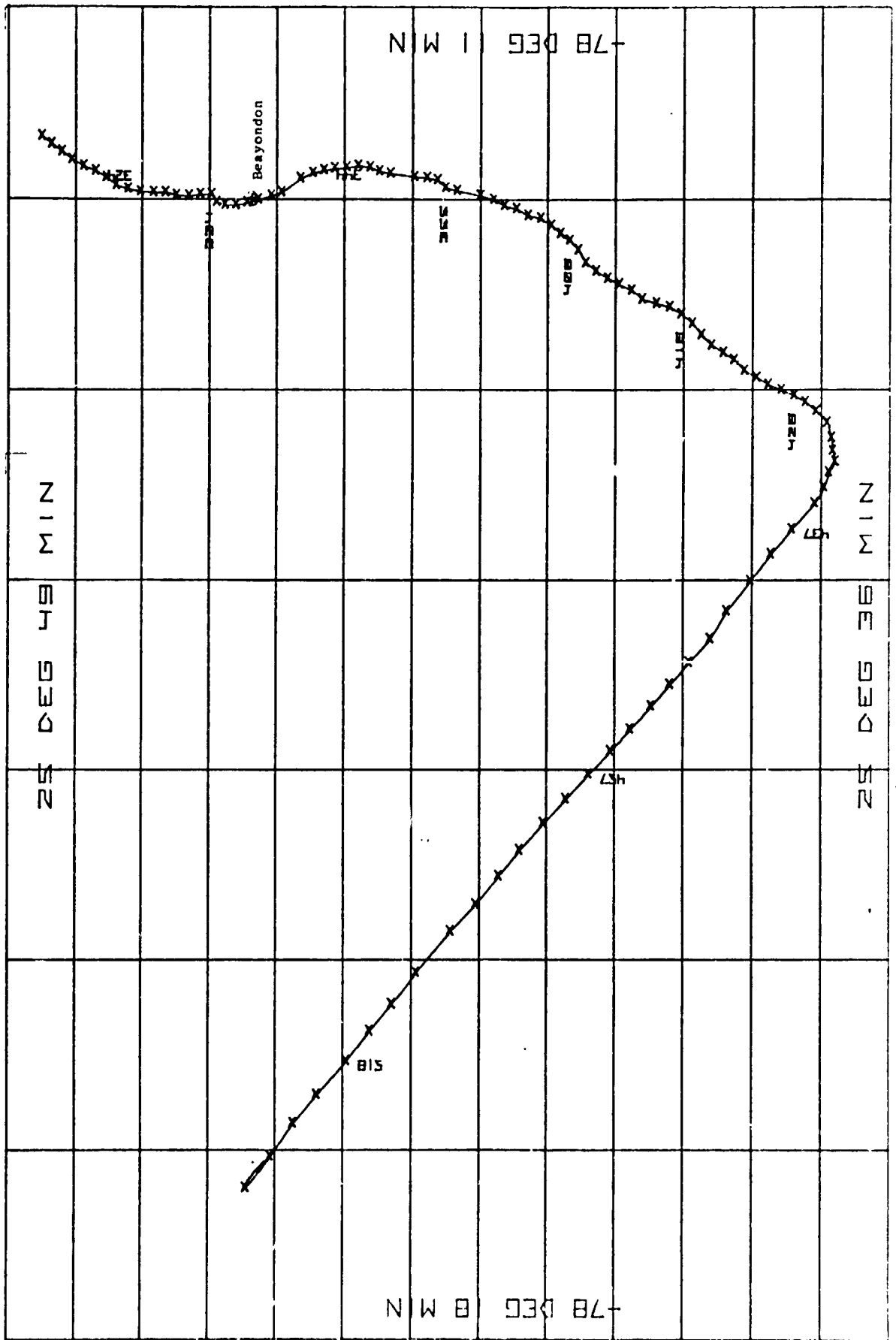


Figure 5

ORIGINAL PAGE IS
OF POOR QUALITY

Table 1

TIME	LATITUDE	LONGITUDE
430	25 33.99900	-76 52.63158
431	25 33.92280	-76 52.49940
432	25 33.84198	-76 52.36596
433	25 33.76026	-76 52.24332
434	25 33.69024	-76 52.12248
435	25 33.59640	-76 51.99294
436	25 33.50580	-76 51.87030
437	25 33.40428	-76 51.75090
438	25 33.32604	-76 51.65346
439	25 33.22800	-76 51.54348
440	25 33.14034	-76 51.44358
441	25 33.05868	-76 51.33672
442	25 32.99706	-76 51.22662
443	25 32.96436	-76 51.14736
444	25 32.94324	-76 51.06990
445	25 32.95290	-76 51.00180
446	25 33.00138	-76 50.95374
447	25 33.05988	-76 50.91324
448	25 33.14532	-76 50.88840
449	25 33.25984	-76 50.88930
450	25 33.38916	-76 50.88012
451	25 33.50436	-76 50.87796
452	25 33.60924	-76 50.88396
453	25 33.71250	-76 50.87742
454	25 33.80880	-76 50.85204
455	25 33.87762	-76 50.82420
457	25 33.94776	-76 50.71770
458	25 33.93798	-76 50.63970
459	25 33.92760	-76 50.55666
500	25 33.90132	-76 50.45478
501	25 33.83204	-76 50.33406
503	25 33.70278	-76 50.11098
504	25 33.69600	-76 50.03742
505	25 33.70818	-76 49.97136
506	25 33.75396	-76 49.93986
517	25 33.81900	-76 49.91838
508	25 33.92568	-76 49.92390
509	25 34.06776	-76 49.94262
511	25 34.35066	-76 50.00904
512	25 34.48948	-76 50.04420
513	25 34.62792	-76 50.08752
514	25 34.75932	-76 50.11452
515	25 34.85742	-76 50.10948
516	25 34.94622	-76 50.10142
517	25 35.00124	-76 50.17558
518	25 35.07492	-76 49.96566
519	25 35.15470	-76 49.87524
521	25 35.04102	-76 49.78290
522	25 34.99518	-76 49.66608
523	25 34.95056	-76 49.54116
524	25 34.89624	-76 49.43862
525	25 34.82444	-76 49.29564
526	25 34.80186	-76 49.16814
527	25 34.77726	-76 49.02534
528	25 34.77424	-76 48.96420
529	25 34.81462	-76 48.90190

Table 1 cont'd

530	25	34.87950	-76	48.86772
531	25	34.96104	-76	48.85716
532	25	35.06352	-76	48.85356
533	25	35.19762	-76	48.87102
535	25	35.47332	-76	48.93516
536	25	35.58744	-76	48.95670
537	25	35.70096	-76	48.97326
538	25	35.82420	-76	48.99738
539	25	35.96886	-76	49.03344
540	25	36.09444	-76	49.05948
541	25	36.21222	-76	49.07736
542	25	36.33456	-76	49.09650
543	25	36.45222	-76	49.11444
544	25	36.55998	-76	49.12482
545	25	36.64902	-76	49.10946
546	25	36.68994	-76	49.06386
547	25	36.72930	-76	49.00578
548	25	36.69216	-76	48.90228
549	25	36.66672	-76	48.80322
550	25	36.64278	-76	48.69858
552	25	36.48444	-76	48.43566
553	25	36.38634	-76	48.30318
554	25	36.28764	-76	48.16572
555	25	36.16884	-76	48.02634
556	25	36.10110	-76	47.92404
557	25	36.00372	-76	47.79666
558	25	35.88342	-76	47.66286
559	25	35.79102	-76	47.53926
600	25	35.70570	-76	47.41878
601	25	35.62920	-76	47.31642
602	25	35.56230	-76	47.20110
603	25	35.51292	-76	47.08332
604	25	35.47338	-76	46.97304
605	25	35.44822	-76	46.87110
606	25	35.48820	-76	46.77486
607	25	35.51274	-76	46.67988
608	25	35.55270	-76	46.58316
609	25	35.56686	-76	46.49382
610	25	35.57214	-76	46.40448
611	25	35.56998	-76	46.32756
612	25	35.52312	-76	46.24800
613	25	35.47296	-76	46.19778
614	25	35.39508	-76	46.16304
615	25	35.30658	-76	46.14198
616	25	35.22864	-76	46.14102
617	25	35.13402	-76	46.14996
618	25	35.03832	-76	46.16712
619	25	34.94136	-76	46.17918
620	25	34.84154	-76	46.18446
621	25	34.75682	-76	46.19292
622	25	34.69812	-76	46.19746
623	25	34.61124	-76	46.19842
624	25	34.54524	-76	46.20714
625	25	34.48798	-76	46.21320
626	25	34.46088	-76	46.23126
627	25	34.41672	-76	46.23612
628	25	34.37004	-76	46.24416
629	25	34.34424	-76	46.26720
630	25	34.32650	-76	46.28950

Table 1 cont'd

633	25	34.29432	-76	46.26078
634	25	34.28988	-76	46.24134
635	25	34.27836	-76	46.21878
636	25	34.28760	-76	46.22130
637	25	34.29384	-76	46.21698
638	25	34.28508	-76	46.19880
639	25	34.30674	-76	46.19262
641	25	34.35126	-76	46.21086
642	25	34.36032	-76	46.23156
644	25	34.38840	-76	46.26228
646	25	34.41864	-76	46.29240
648	25	34.44672	-76	46.32318

ORIGINAL PAGE IS
OF POOR QUALITY

ORIGINAL PAGE IS
OF POOR QUALITY

Table 2

TIME	LATITUDE	LONGITUDE
1035	25 34.16556	-76 46.90632
1036	25 34.27326	-76 46.88232
1037	25 34.38096	-76 46.85832
1038	25 34.48866	-76 46.83432
1039	25 34.60068	-76 46.80414
1040	25 34.71270	-76 46.77594
1041	25 34.82634	-76 46.74546
1051	25 35.99772	-76 46.39968
1052	25 36.09744	-76 46.38324
1053	25 36.18480	-76 46.36998
1054	25 36.26664	-76 46.35372
1055	25 36.31536	-76 46.36230
1056	25 36.33546	-76 46.37202
1057	25 36.32844	-76 46.38510
1058	25 36.29178	-76 46.40190
1059	25 36.22998	-76 46.41960
1100	25 36.15084	-76 46.44114
1101	25 36.05454	-76 46.46202
1102	25 35.94300	-76 46.48068
1103	25 35.82336	-76 46.50348
1104	25 35.69874	-76 46.53066
1105	25 35.57484	-76 46.56240
1106	25 35.45064	-76 46.59726
1107	25 35.32116	-76 46.63176
1108	25 35.19342	-76 46.67124
1109	25 35.07180	-76 46.71756
1110	25 34.95438	-76 46.76520
1111	25 34.84062	-76 46.80924
1112	25 34.73706	-76 46.85112
1113	25 34.64904	-76 46.89264
1114	25 34.57494	-76 46.93122
1115	25 34.51926	-76 46.96860
1116	25 34.47504	-76 46.99794
1117	25 34.44588	-76 47.01924
1118	25 34.43160	-76 47.03922
1119	25 34.42128	-76 47.05254
1120	25 34.41120	-76 47.05914
1121	25 34.40904	-76 47.06260
1122	25 34.40808	-76 47.05962
1123	25 34.41522	-76 47.05794
1124	25 34.42818	-76 47.05980
1125	25 34.44966	-76 47.06454
1125	25 34.47912	-76 47.07229
1127	25 34.50852	-76 47.08702
1130	25 34.59684	-76 47.10324

ORIGINAL PAGE IS
OF POOR QUALITY

Table 3

TIME	LATITUDE	LONGITUDE
319	25 48.50892	-78 11.68164
320	25 48.34800	-78 11.71710
321	25 48.18702	-78 11.75256
322	25 48.02610	-78 11.78802
323	25 47.86410	-78 11.82222
324	25 47.69850	-78 11.85372
325	25 47.52768	-78 11.88150
327	25 47.17698	-78 11.92578
328	25 47.00256	-78 11.94354
329	25 46.82724	-78 11.95884
330	25 46.65108	-78 11.96952
331	25 46.47468	-78 11.97342
332	25 46.31406	-78 11.98110
333	25 46.16304	-78 11.99040
334	25 46.01448	-78 11.99970
335	25 45.86556	-78 12.00456
336	25 45.71964	-78 12.00696
337	25 45.56994	-78 12.00810
338	25 45.42054	-78 12.00648
339	25 45.24192	-78 11.98890
340	25 45.05526	-78 11.96496
341	25 44.86794	-78 11.93910
342	25 44.68188	-78 11.91402
343	25 44.49378	-78 11.89020
344	25 44.30934	-78 11.86764
345	25 44.12358	-78 11.84910
346	25 43.95612	-78 11.84364
347	25 43.79226	-78 11.84394
348	25 43.62600	-78 11.84784
349	25 43.45578	-78 11.85285
350	25 43.28904	-78 11.86038
352	25 42.96360	-78 11.88630
353	25 42.80424	-78 11.90202
354	25 42.63936	-78 11.91624
355	25 42.46926	-78 11.93046
356	25 42.30378	-78 11.94484
358	25 41.97162	-78 11.98848
359	25 41.80350	-78 12.01206
400	25 41.62674	-78 12.03216
401	25 41.45256	-78 12.05502
402	25 41.29312	-78 12.08322
403	25 41.12304	-78 12.11364
404	25 40.96656	-78 12.14616
405	25 40.82016	-78 12.18711
406	25 40.67640	-78 12.22811
407	25 40.53504	-78 12.27360
408	25 40.39260	-78 12.31758
409	25 40.24314	-78 12.36006
410	25 40.09038	-78 12.40422
411	25 39.92510	-78 12.44436
412	25 39.77010	-78 12.47766
413	25 39.57436	-78 12.50998
414	25 39.39216	-78 12.54096
415	25 39.22044	-78 12.58218
416	25 39.05358	-78 12.62370
417	25 38.88426	-78 12.66346

Table 3 cont'd

418	25	38.72375	-78	12.70652
419	25	38.56944	-78	12.75450
420	25	39.41356	-78	12.80256
421	25	39.25578	-78	12.84870
422	25	38.09214	-78	12.89022
423	25	37.92090	-78	12.92808
424	25	37.75116	-78	12.96528
425	25	37.58040	-78	13.00380
426	25	37.40910	-78	13.04298
427	25	37.25358	-78	13.08816
428	25	37.11996	-78	13.13796
429	25	37.00812	-78	13.19190
430	25	36.93678	-78	13.24950
431	25	36.89368	-78	13.31364
432	25	36.90186	-78	13.38300
433	25	36.96240	-78	13.45308
434	25	37.04826	-78	13.52052
435	25	37.14900	-78	13.58772
437	25	37.2284	-78	13.72944
439	25	37.31564	-78	13.87524
441	25	38.01534	-78	14.01720
443	25	38.31438	-78	14.15340
445	25	38.60580	-78	14.28672
447	25	38.89812	-78	14.41878
449	25	39.18924	-78	14.54718
451	25	39.47754	-78	14.67000
453	25	39.77052	-78	14.79060
455	25	40.08450	-78	14.91144
457	25	40.40058	-78	15.03528
459	25	40.72176	-78	15.16356
461	25	41.04702	-78	15.29496
463	25	41.38434	-78	15.43000
465	25	41.72340	-78	15.56914
467	25	42.06432	-78	15.71232
469	25	42.40700	-78	15.85764
472	25	42.71632	-78	16.00922
474	25	43.27422	-78	16.23306
476	25	43.63256	-78	16.38662
478	25	43.98678	-78	16.54494
480	25	44.34664	-78	16.70682
482	25	44.63456	-78	16.84434
484	25	44.92100	-78	16.99212
486	25	45.32304	-78	17.13984
488	25	45.65500	-78	17.28762

ORIGINAL PAGE IS
OF POOR QUALITY

ORIGINAL PAGE IS
DE POOR QUALITY

Table 4

TIME	LATITUDE	LONGITUDE
425	25 50.94618	
427	25 50.59696	-78 2.49240
428	25 50.40732	-78 2.60508
429	25 50.22774	-78 2.66142
430	25 50.06460	-78 2.71776
432	25 49.73688	-78 2.78154
433	25 49.57668	-78 2.89548
435	25 49.27866	-78 2.95080
436	25 49.12452	-78 3.06744
437	25 48.97644	-78 3.12048
438	25 48.82764	-78 3.17352
439	25 48.65982	-78 3.22542
440	25 48.49170	-78 3.26568
441	25 48.32466	-78 3.30594
442	25 48.14172	-78 3.34524
443	25 47.97828	-78 3.37350
444	25 47.81106	-78 3.41346
445	25 47.63664	-78 3.45066
446	25 47.46288	-78 3.47850
447	25 47.28180	-78 3.50544
448	25 47.09910	-78 3.52312
449	25 46.92570	-78 3.55044
450	25 46.73280	-78 3.57804
451	25 46.53420	-78 3.59166
452	25 46.34940	-78 3.60144
453	25 46.18074	-78 3.62202
454	25 46.02840	-78 3.65292
455	25 45.86772	-78 3.69264
456	25 45.71010	-78 3.72546
457	25 45.56172	-78 3.76056
458	25 45.42978	-78 3.80166
459	25 45.29196	-78 3.85374
500	25 45.13590	-78 3.90276
501	25 44.97000	-78 3.93894
502	25 44.80050	-78 3.97074
503	25 44.62740	-78 4.00794
504	25 44.45040	-78 4.03302
505	25 44.26956	-78 4.06206
506	25 44.07204	-78 4.08762
507	25 43.87818	-78 4.10358
508	25 43.68864	-78 4.12464
509	25 43.49922	-78 4.14618
510	25 43.31458	-78 4.16772
511	25 43.11876	-78 4.19442
512	25 42.92376	-78 4.20960
513	25 42.76410	-78 4.22790
514	25 42.62412	-78 4.26348
515	25 42.50932	-78 4.30350
516	25 42.41868	-78 4.35066
517	25 42.36216	-78 4.40244
518	25 42.36318	-78 4.46094
519	25 42.40074	-78 4.53552
520	25 42.46884	-78 4.61454
521	25 42.56444	-78 4.69572
522	25 42.68244	-78 4.78326
523	25 42.82094	-78 4.87356
		-78 4.96572

Table 4 cont'd

524	25	42.99504	-78	5.07510
525	25	43.17696	-78	5.18790
526	25	43.35036	-78	5.29674
527	25	43.51422	-78	5.40246
528	25	43.67112	-78	5.50536
529	25	43.82874	-78	5.60808
530	25	43.98126	-78	5.70678
531	25	44.11248	-78	5.79474
532	25	44.22786	-78	5.87370
533	25	44.35572	-78	5.95794
534	25	44.49258	-78	6.04542
535	25	44.63430	-78	6.13398
536	25	44.78100	-78	6.22440
537	25	44.92584	-78	6.31446
538	25	45.07098	-78	6.40596
539	25	45.22014	-78	6.49878
540	25	45.36048	-78	6.58764
541	25	45.49122	-78	6.67128
542	25	45.61836	-78	6.75348
543	25	45.73470	-78	6.83076
544	25	45.84732	-78	6.90444
545	25	45.96360	-78	6.97800
546	25	46.07940	-78	7.05318
547	25	46.20246	-78	7.13484
548	25	46.33512	-78	7.22250
549	25	46.46952	-78	7.31046
550	25	46.61616	-78	7.40526
551	25	46.77066	-78	7.50570
552	25	46.93098	-78	7.61004
553	25	47.09736	-78	7.71594
554	25	47.26374	-78	7.81668
555	25	47.41494	-78	7.90896
556	25	47.56320	-78	8.00124
557	25	47.70740	-78	8.08812
558	25	47.83800	-78	8.17584
559	25	47.95128	-78	8.25600
600	25	48.04998	-78	8.33724
601	25	48.12882	-78	8.42070
602	25	48.19830	-78	8.51148
603	25	48.23952	-78	8.59902
604	25	48.25180	-78	8.68312
605	25	48.21312	-78	8.76462
606	25	48.14400	-78	8.83716
607	25	48.05010	-78	8.90418
608	25	47.93136	-78	8.96424
609	25	47.77914	-78	9.01266
610	25	47.61678	-78	9.05108
611	25	47.44544	-78	9.10416
612	25	47.27736	-78	9.15024
613	25	47.10162	-78	9.19212
614	25	46.91358	-78	9.22932
615	25	46.71156	-78	9.26004
616	25	46.52310	-78	9.29514
617	25	46.32330	-78	9.32316
618	25	46.12842	-78	9.35376
619	25	45.93018	-78	9.38682
620	25	45.76512	-78	9.42912
621	25	45.54694	-78	9.47070

ORIGINAL PAGE IS
OF POOR QUALITY

ORIGINAL PAGE IS
OF POOR QUALITY

Table 4 cont'd

622	25	45.45103	-78	9.52440
623	25	45.30474	-78	9.57900
624	25	45.17754	-78	9.64260
625	25	45.04248	-78	9.70278
626	25	44.90466	-78	9.76140
627	25	44.75412	-78	9.81402
628	25	44.60754	-78	9.86808
629	25	44.43822	-78	9.91134
630	25	44.25642	-78	9.94794
631	25	44.05824	-78	9.97632
632	25	43.85538	-78	10.00128
633	25	43.65606	-78	10.02552
634	25	43.45668	-78	10.04892
635	25	43.25412	-78	10.06968
637	25	42.86670	-78	10.11750
638	25	42.68244	-78	10.14444
639	25	42.49206	-78	10.16760
640	25	42.30294	-78	10.19010
641	25	42.10530	-78	10.20850
642	25	41.90394	-78	10.22418
643	25	41.69892	-78	10.23690
644	25	41.50236	-78	10.25364
645	25	41.29254	-78	10.26438
646	25	41.08062	-78	10.27306
647	25	40.85808	-78	10.27722
648	25	40.59060	-78	10.25760
649	25	40.28814	-78	10.21968
650	25	39.95628	-78	10.16736
651	25	39.58356	-78	10.09512
652	25	39.19188	-78	10.01214
653	25	38.77314	-78	9.91572
654	25	38.39610	-78	9.84126
655	25	38.07048	-78	9.79332
656	25	37.79250	-78	9.77052
657	25	37.55262	-78	9.76752
658	25	37.37076	-78	9.79182
659	25	37.22586	-78	9.83550
700	25	37.15446	-78	9.90636
701	25	37.09602	-78	9.97542
702	25	37.05462	-78	10.04466
704	25	37.13334	-78	10.18662
705	25	37.16754	-78	10.25418
706	25	37.22714	-78	10.31250
709	25	37.52392	-78	10.45788
710	25	37.70292	-78	10.47006
711	25	37.84050	-78	10.47678
712	25	38.04286	-78	10.47774
713	25	38.15418	-78	10.44594
714	25	38.30484	-78	10.40382
715	25	38.45494	-78	10.36032
716	25	38.63340	-78	10.31718
717	25	38.79030	-78	10.27302
718	25	38.95924	-78	10.22922
719	25	39.11592	-78	10.18632
720	25	39.27020	-78	10.14546
721	25	39.42546	-78	10.10478
722	25	39.57372	-78	10.06398
723	25	39.72164	-78	10.02540

ORIGINAL PAGE IS
OF POOR QUALITY

Table 4 cont'd

724	25	39.88446	-78	9.99480
725	25	40.05342	-78	9.96726
726	25	40.23642	-78	9.94626
727	25	40.42450	-78	9.92892
728	25	40.62768	-78	9.91500
729	25	40.82166	-78	9.89820
730	25	40.99806	-78	9.87126
731	25	41.16234	-78	9.83880
732	25	41.33022	-78	9.80850
733	25	41.48604	-78	9.77268
734	25	41.64276	-78	9.73668
735	25	41.78478	-78	9.69510
736	25	41.93868	-78	9.65898
737	25	42.11076	-78	9.63294
738	25	42.28378	-78	9.60924
739	25	42.44844	-78	9.57708
740	25	42.60528	-78	9.54330
741	25	42.74784	-78	9.50310
742	25	42.89910	-78	9.46608
743	25	43.04616	-78	9.42708
744	25	43.18722	-78	9.38418
745	25	43.32726	-78	9.34158
746	25	43.47852	-78	9.30384
747	25	43.63398	-78	9.26392
748	25	43.79784	-78	9.23802
749	25	43.96098	-78	9.20730
750	25	44.12430	-78	9.17652
751	25	44.28726	-78	9.14580
752	25	44.45160	-78	9.11484
753	25	44.61684	-78	9.08358
754	25	44.77776	-78	9.05334
755	25	44.94114	-78	9.02292
756	25	45.10452	-78	8.99250
757	25	45.26790	-78	8.96208

OCEAN BATHYMETRY ANALYSIS AND POSITION SUMMARY
PHASE I

Approx. Time of Occupancy	Location	Beyondan Position		Predicted Precision of Beyondan Position	Calypso Position		LORAN C		Station Number
		Latitude	Longitude		Latitude	Longitude	Measured-Jupiter Nautucket	Grid Bias Computed Nautucket	
24 Aug 1200-26 Aug 2300	Nassau	25° 4.765'	77° 20.255'	15 Meters	-	-	+1	-0.3	19
27 Aug 0600-27 Aug 0730	Off Eleuthera	25° 32.801'	76° 51.267'	100 Meters	-	-	0	0	1
27 Aug 0800-27 Aug 1730	"	25° 34.712'	76° 46.422'	15 Meters	25° 34.5216'	76° 46.3192'	+2	-0.5	2
Calypso - after Transit					25° 34.8568'	76° 47.0645'			5
28 Aug 0300-28 Aug 0400	Berry Islands	25° 45.367'	78° 12.003'	100 Meters	-	-	+1	Unlocked	1
28 Aug 0500-28 Aug 1200	"	25° 47.743'	78° 15.783'	38 Meters	25° 47.6411'	78° 19.8336'	-0.2	-0.3	4
28 Aug 1300-28 Aug 2200	"	25° 42.870'	78° 28.011'	43 Meters	25° 42.7710'	78° 28.1331'			3
28 Aug 2312-29 Aug 0300		25° 50.859'	78° 31.828'	52 Meters	-	-			4
29 Aug 0700-29 Aug 0913		26° 2.0915'	78° 56.736'	50 Meters	20° 1.9746'	78° 56.8082'			2
29 Aug 1202-29 Aug 1330	Great Isaac Light	26° 2.0486'	79° 5.7586'	81 Meters	-	-			3
29 Aug 1400-29 Aug 2030		26° 00.027'	79° 11.485'	46 Meters	25° 57.31'	79° 12.24'			10
Evening Anchorage of Calypso		-	-	-	25° 59.980'	79° 11.6196'			
30 Aug 0700-30 Aug 0920		26° 2.330'	80° 5.766'	74 Meters					3
30 Aug 1002-30 Aug 1200		26° 3.873'	80° 5.671'	36 Meters	26° 3.8556'	80° 5.648'			2

ORIGINAL PAGE IS
OF POOR QUALITY

Table 5

OCEAN BATHYMETRY ANALYSIS AND POSITION SUMMARY
 PHASE II

Approx. Time of Occurrence	Location	Bayandan Position Latitude Longitude	Predicted Precision of Bayandan Position	Calypso Position Latitude Longitude	LORAN C Grid Bias Measured-Computed Jupiter-Nantucket μSEC	Number Number of Transit Passes	Station Number
4 Sept 2200-5 Sept 0700	Little Bahama Bank	27° 6.669' 78° 53.808'	26 Meters	27° 6.6302' 78° 53.367'	+1 +.07	6	20
5 Sept 1000-5 Sept 1430	Whiting Plume	27° 3.5130' 78° 54.1408'	40 Meters	27° 4.954' 78° 55.152'	+2 -.2	4	21
6 Sept 0500-6 Sept 1100	Berry Islands	25° 45.2604' 78° 8.9530'	41 Meters	25° 45.116' 78° 9.011'	+1 -.2	5	22
6 Sept 1300-7 Sept 1600	"	25° 46.77' 78° 25.179'	80 Meters	25° 46.668' 78° 25.2614'	-.1 -.3	1	23
6 Sept 1630-7 Sept 1000 After Transit	"	25° 48.879' 78° 27.2446'	25 Meters	25° 48.906' 78° 27.105'	+3 -.4	7	24
7 Sept 1500-7 Sept 1600	Little Isaac	25° 58.201' 78° 52.789'	90 Meters	25° 48.998' 78° 27.087'	+18 -.1	1	25
7 Sept 1800-7 Sept 2100	Great Isaac	25° 59.005' 79° 11.570'	80 Meters	25° 59.0677' 79° 11.561'	+3 -.6	2	26

ORIGINAL PAGE IS
 OF POOR QUALITY

Table 6



FORMERLY WILLOW RUN LABORATORIES THE UNIVERSITY OF MICHIGAN

ORIGINAL PAGES
OF POOR QUALITY

APPENDIX B

Technical Memorandum RSC-131

WHITING INVESTIGATIONS ON THE LITTLE
BAHAMAS BANK

March 1976

Texas A&M University
Remote Sensing Center

Technical Memorandum RSC-131
Whiting Investigations on the
Little Bahamas Bank

John M. Hill*, Fabian C. Polcyn**, and Charles Vermillion***

INTRODUCTION

An investigation in the Bahamas to evaluate the capability of the high gain mode of Landsat 1 and 2 to determine bathymetric data included an investigation of an anomaly called Whittings. The Whiting Investigation was conducted by NASA/Goddard Space Flight Center, the Environmental Research Institute of Michigan, the Remote Sensing Center of Texas A&M University, the Applied Physics Laboratory of Johns Hopkins University, the U.S. Coast Guard, and the Cousteau Society.

The whittings were observed in satellite images even before the ship sailed. The whittings were investigated because they could conceivably cause an alarm due to their similarity to shoal areas.

BACKGROUND ON POSSIBLE ORIGINS OF WHITINGS

Shallow-water sedimentation is a complicated process. It involves chemical, physical and biological

-
- * Remote Sensing Center, Texas A&M University, College Station, Texas, 77843, U.S.A.
 - ** Environmental Research Institute of Michigan, P.O. Box 618, Ann Arbor, Michigan, 48107, U.S.A.
 - *** NASA/Goddard Space Flight Center, Greenbelt, Maryland, 20771, U.S.A.

relationships. The solubility of CaCO_3 changes with varying levels in photosynthesis, respiration, precipitation of CaCO_3 , evaporation, rainfall and fresh water run-off from the shoreline (Bathurst, 1975). Organisms not only secrete carbon skeletons; they are also a prime factor in breaking and stirring them up. Tidal and wind-driven currents as well as wave action are the main factors in the abrasion and dissemination of these particles.

The Little Bahama Bank, adjacent to the island of Grand Bahama, is similar to the Grand Bahama Bank in that it is a large flat bank surrounded and sheltered by rocky shoals. This creates an area of relatively undisturbed water. Water movement is important in the supplying of nutrients to biological communities and has an influence on the distribution of carbonate which can be in solution (Smith, 1940; Costin, 1965; B. Katz, 1965, Traganza, 1967). Bathurst (1975) explains that tidal movements can be easily modified by winds. From March or April to the end of August the prevailing winds are generally from the east or southeast and in September they begin to move toward the north.

Surface water temperatures from 22°C to 31°C (February-August) are attributed to warm waters brought to the Bahamas by the Gulf Stream (Smith, 1940; Cloud, 1962; Broecker and Takahashi, 1968) and to insulation on the shallow banks. Cloud (1962) found that the lateral

variation on the Great Bahama Bank was only about 0.5°C. The water in these shallow areas is relatively well mixed by the wind.

Whitings consist of suspended aragonite muds that appear as clouds of milk-white water. The origin of aragonite muds which make up whitings is currently under question and examination. Some investigators believe these muds to be accumulations of aragonite needles from decomposed codiacean and dasycladacean algae (Lowenstam and Epstein, 1975; Stockman, Ginsburg and Shinn, 1967; Neumann and Land, 1969).

Cloud (1962) conducted an investigation on the environment of calcium carbonate deposition west of Andros Island, Bahamas which included a study of whitings. He states that the propeller and dragging anchor of his ship, the Physalia, made whitings as they stirred up the bottom. Underwater springs as well as outbursts of gas can cause similar conditions. Cloud also states that unusual local meteorological conditions may also produce identical effects. Ginsburg (1956) observed similar clouds of sediment which were stirred up by schools of bottom feeding fish, such as mullet. These plumes are termed "fish muds" and were observed in Florida Bay. Wells and Illing (1964) investigated whitings in the Persian Gulf which they believe to

be related or similar to those found in the Bahamas. They observed that the milky patches, or whittings, appeared and grew within a few minutes and persisted in the area for several hours. The visibility in these whittings was from less than 0.5 m to a few centimeters, the suspension consisted of aragonite needles and some pelagic organisms, and the density was approximately 1g of solid/100L. The following, although these observations sound as if the tail of a whiting instead of the source had been observed, are some interesting points made by Wells and Illing:

- (1) The milkiness appears at the same moment over an area of many square kilometres. The region is normally devoid of fish which, even where they disturb the bottom, only muddy the water in patches a few hundred meters across.
- (2) The whittings form at the surface and overlies clear water.
- (3) They occur over any depth of water in the Gulf but are very frequent, though smaller, over depths of less than 10 m.
- (4) The aragonite crystals flocculate, sink and disappear from sight in less than a day, whereas stirred bottom mud takes several days to settle.

- (5) The underlying bottom mud contains up to 50% calcite, but in the whiting there is "very little calcite".
- (6) Analysis of water immediately before and after the appearance of a whiting suggests that there is a very slight drop in Ca^{2+} and $\text{Ca}^{2+}/\text{Mg}^{2+}$. This could mean that calcium had been removed from the solution.
- (7) Water stratification in terms of temperature, salinity and pH remains stable and this points to the absence of turbulence and bottom disturbance.

Bahamian aragonite mud can be formed by either inorganic or organic (physiological) processes. Stockman et al. (1967) have found that the algae are adequate sources of recent aragonite mud. A fact that is confusing is that there exist areas of sheltered waters such as in the Bimini Lagoon that have prolific algal blooms with no aragonite muds (Bathurst, 1975).

Cloud (1962) estimated that 5 wt. % of the mud is detrital, 17-20 wt. % is skeletal remains, of which 4-5% is algal aragonite, therefore leaving 75 wt. % to be accounted for by some other process. This has led to the possibility of inorganic precipitation. Black (1933) concluded that in shall areas west of Andros Island the high rate of evaporation

generates a high concentration of salts, when in combination with the loss of CO_2 , causes precipitation of tiny aragonite crystals. Smith (1940) and Cloud (1962) showed that rates of withdrawal of CaCO_3 were related to an increase of residence time of the water on the banks, as well as to the salinity and the accompanying fall in the produced $\text{Ca}^{2+} \cdot \text{CO}_3^{2-}$ as aragonite is precipitated. Broecker and Takahashi (1966) state that the rate of CaCO_3 precipitation is proportional to the degree of supersaturation. This data would tend to justify the inorganic origin of the aragonite muds. For this relationship does not necessarily have to exist if the process is biological. They, however, could not account for a large percentage of the CO_2 budget which is lost from the Bank. It is assumed that the CO_2 must be removed from the Bank and is lost to the deep ocean.

Another hypothesis (Weyl, 1961) is that in sea water saturated for aragonite, a sudden bloom of diatoms can remove so much CO_2 from the water that the only way to reach an equilibrium is by a widespread precipitation of CaCO_3 , thus causing whittings. DeGroot (1965), however, conducted laboratory experiments which tend to disprove Wells' and Illing's hypothesis. His findings indicated that sudden appearances of whittings in the Persian Gulf could not have occurred because the maximum rate of precipitation of aragonite from sea water is much too slow.

Even when hurried up in the laboratory, it still took at least two weeks to form a precipitate.

Aragonite needle precipitates occurring at intervals of a few years also occur in the surface waters of the Dead Sea. Neev and Emery (1967) investigated one in which the suspended HCO_3^- concentrations first occurred at the surface and progressed downward to a maximum depth of 40 m. The bottom sediments were found to consist of the heavier isotopes O^{18} and C^{13} . The precipitation of HCO_3^- at the near surface, due to evaporation, would cause the selective loss of lighter oxygen and carbon isotopes. Their data also favors the hypothesis of aragonite precipitation, but one should keep in mind that the water in the Dead Sea is not normal sea water. The extremely high salinities, which far exceed those found in either the Bahamas or Persian Gulf, could very well cause precipitation of HCO_3^- in the surface layers. Revelle and Fairbridge (1957) suggested that temporary morning clouding in still waters in the lagoon of Houtman's Abrolhs (southwestern Australia) might be due to photosynthetic reduction of CO_2 pressure.

Cloud (196?) studied three whittings just west of Andros Island. The first whiting drifted away before it could be entered, but an underwater inspection of the drifting margin proved the water to be unusually milky due to suspended matter. No local turbulences or bottom disturbances were noted at the site.

C-2

Upon entering the second whitening, Cloud states that "its center gave the sensation of weightless fixity in the middle of a sunlit cloud band. It was impossible without resting motionless, to detect buoyancy and drift or to tell up from down or sideways. The brilliant lighting was so dispersed that a hand, invisible at arm's length, had to be extended to grope for bottom and avoid a collision on surfacing. No fish were seen (or felt) nor was any other evidence of bottom disturbance found". The suspended material, upon microscopic examination, was found to consist of primarily aragonite needles.

The third whitening was about 4 km long and 0.8 km wide. During a six-hour study no large schools of fish were observed except for a few small Halichoeres, tiny Eques found in and about the sponges and much later five sharks were seen. No other whitenings were seen to occur in the surrounding area. Chemical analyses of water samples from inside and outside the whitenings were examined. The whitening water, after particles larger than 0.45 microns were filtered out, was significantly high in calcium, phosphates, CO_2 evasion, pH, the rate of photosynthesis, and low in alkalinity and partial pressure of CO_2 . The whitening kept its properties for at least 45 hours without being eliminated by diffusion or from mixing caused by external sources.

Cloud noted that all of the whittings were elongated and drifted with the wind and tidal current. No schooling of fish was observed in the area, the whittings did not drift away from a fixed point or move around erratically, and no unusual meteorological or other disturbances were noted. He made no definite conclusions as to the specific cause or origin of these whittings except for the mentioning of the possibility of the previously stated ideas of inorganic or biological processes.

Cloud stressed the need to examine individual whittings in any given area to determine what features they either have in common or in which they differ.

WHITING OBSERVATIONS AS COLLECTED FROM THE CALYPSO

Two whittings were investigated by the scientists and crew of the R/V Calypso on the fifth of September, 1975 on the Little Bahama Bank. Whittings occurring in this area were observed in satellite images even before the cruise.

Upon entering the area, a T-38 aircraft was utilized to obtain a synoptic view of the area and to locate a group of whittings. Once the area of whittings had been identified by the jet, the Calypso was directed to the source of the whiting by the Calypso helicopter. A Zodiac, a small rubber raft, was deployed from the ship and sent to the source.

Upon arriving at the source the Zodiac was anchored and the divers proceeded to enter the whiting. The Zodiac was used because of its speed, maneuverability, and it lessened the chance that schools of fish would be scared away if present. The excellent naturalistic instincts and experience of Captain Cousteau's divers made it possible for several new and interesting observations.

The Zodiac crew collected measurements of depth, secchi depth, sea surface temperature, surface salinity, and water samples for later analysis. The divers collected bottom temperature, bottom salinity, water samples, sediment samples (Figure 1) depth vertical visibility, horizontal visibility, current direction, a rough estimation of current speed and general bottom descriptions and comments (Table 1). Water and sediment samples and observations were collected from the source, the tail, and from the clear water surrounding the whittings.

The source of the first whiting, Station EB, had several sharks swimming within it. One shark even took a swipe at a diver's flipper. Investigators have been known to not enter the whittings for just such a reason. Once in the plume the divers observed Callianassa mounds, with heights of 6 to 10 centimeters, covering the bottom (Figure 2). Bathurst (1975) states that conical mounds constructed by Callianassa, burrowing shrimp, are common in stable sand

ORIGINAL PAGE IS
OF POOR QUALITY



Fig. 1. Diver collecting sediment samples for later analysis. Note the very fine sediments. (Courtesy of Joe Thompson and the Cousteau Society)



Fig. 2. Callianassa mounds surrounded by blades of Thalassia. (Courtesy of Joe Thompson and the Cousteau Society)

TABLE 1. Data Obtained from the Whiting Investigation on the Little Bahama Bank by the R/V Calypso (September 5, 1975)

	EB Source	EA Out of Whiting	FC Source	ED Tail
Depth (m)	7.5	7.0	6.5	7.0
Secchi (m)	7.0	Seen on bottom	3.75	4.25
Surf. Temp. (°C)	29.93	29.94	30.98	31.20
Bot. Temp. (°C)	29.90	30.13	30.24	30.19
Surf. Sal. (‰)	38.294	38.307	38.457	38.348
Bot Sal. (‰)	38.316	38.319	38.454	38.342
Vert. Vis. (m)	2.0	7.0	1.0	2.0
Hor. Vis. (m)	0.5	5.0	2.0	2.0
Cur. Dir.	Minimal	S.E.	S.E.	S.E.
Cur. Sp. (knts)	Minimal	0.25	0.75	2.00
Mounds	Present	Present	Present	Present
Sharks	Present	None Observed	None Observed	None Observed
Fish	Present	None Observed	None Observed	None Observed
Meteorological Disturbances	None Observed	None Observed	None Observed	None Observed

habitats. The usual mounds resemble miniature volcanic cones, have remarkably constant sizes, have a basal diameter of about 20 cm, a height of about 6 cm, and have approximately 30° sloping sides. At the peak of the mound there is a vent about 3 mm wide. The cone has a surface of loose sand. Grain have occasionally been seen being expelled from the exhalant vent. Shinn (1968) originally discovered that the mounds were constructed by the crustacean Callianassa. The bases of the closely arranged mounds were surrounded by blades of Thalassia.

Ginsburg (1975) explained that these shrimp homogenize the sand to a point where "the history of deposition and with it the story of successive sea-floor environments is hopelessly jumbled". Bathurst (1975) remarks that in some areas the mounds are the only source of loose grains. Tidal currents derived from evidence obtained around the Berry Islands can move the loose grains about 3 to 4 cm at the most and with time, that could be significant.

A large school of what was termed Bone fish were seen bouncing off the bottom. These fish most probably had attracted the sharks into the area. The fish could have been either bottom feeding or merely cleaning parasites or other growths from their undersides. In this particular area of the whiting, the source was covered with a clear surface

layer approximately 2 m thick. The surface currents, usually being more rapid than bottom currents, could have kept the sediments from rising to the surface at the source. The sediments in the tail of the whiting would eventually disperse into the surface layers. The water was turbid from this clear layer all the way to the bottom.

A diver that had left the Calypso, which was anchored near the middle of the whiting, observed relatively large amounts of sediments being expelled from the Callianassa mounds. This observation raises the question as to whether or not the Callianassa may be a possible cause of whittings.

In the clear water surrounding the source of the same whiting, Station EA, the bottom was again covered with closely arranged Callianassa mounds surrounded by Thalassia blades. No sharks, fish school, or burrowing shrimp were seen disturbing the bottom sediments. New sources of whittings were observed by the crew of the helicopter. The new sources appeared as billowing, or mushrooming clouds of white milky sediments that were being forced to the surface. From searching the literature this is quite possibly the first actual observation of the evolution of a non man-induced whiting in the middle of a shallow bank. It is very difficult to imagine what mechanism might mushroom bottom sediments to the surface in about 7 m of water. That is, in fact, if

the sediments do actually come from the bottom. The large sharks which were observed in the source area of the first whiting could have created a turbulence in the water column. Rezak (1976), in conjunction with the Shell Development Corporation, has studied sediments collected from whittings in the Persian Gulf with an electron microscope. His findings were that the sediments consisted of primarily aragonite needles and fine, fine fragments of mollusk shells which had to be stirred up from the bottom. Currents roughly measured in the whittings ranged from about 0.25 to 0.75 knots. At one station the current was negligible. These values are about the expected for the area. The salinities both top and bottom ranged from a mean of 38.358‰ to 38.352‰ respectively. These summer values are rather high when compared to open ocean waters which are usually around 36‰, but values of 46‰ have been recorded just off Andros Island (Cloud, 1962). The temperature and salinity values point out that the water mass was fairly well mixed from top to bottom and that the possibility of underwater springs, that could have caused these particular whittings, was not probable.

Station EC was located at the source of the second whiting. This was the most dense whiting source because the secchi depth was only 3.75 m. The bottom was again found to be covered with mounds and surrounded by Thalassia grass.

The sediments between the mounds appeared to be darker than the previous area. No sharks, schools of fish, or shrimp were observed stirring up the sediments. The absence of any of the previously observed sources of disturbance from the first whiting left speculation. No meteorological disturbances were observed in the local area over either of the two whittings investigated.

Station ED was established to investigate the tail of the second whiting. The sediments were still quite concentrated even when about 1 km from the source since the secchi depth was 4.25 m. The mounds surrounded by grass were again observed. No sharks, fish, or shrimp were seen in the tail of the plume of the second whiting.

The general shape of these whittings can be constructed from the observations (Figure 3). A layer of clear water was over the source of the first whiting. The sediments were also the most dense from top to bottom in the source of both whittings. The vertical visibility observations made on the bottom, in the tails of both whittings, especially in the first whiting since it was most probably the oldest and longest of the two, was much better. The better bottom visibility and the lack of a clear surface layer would lead to the belief that the heavier sediments have already settled out and that the finer particles are carried to the surface layers in the tail of the whittings.

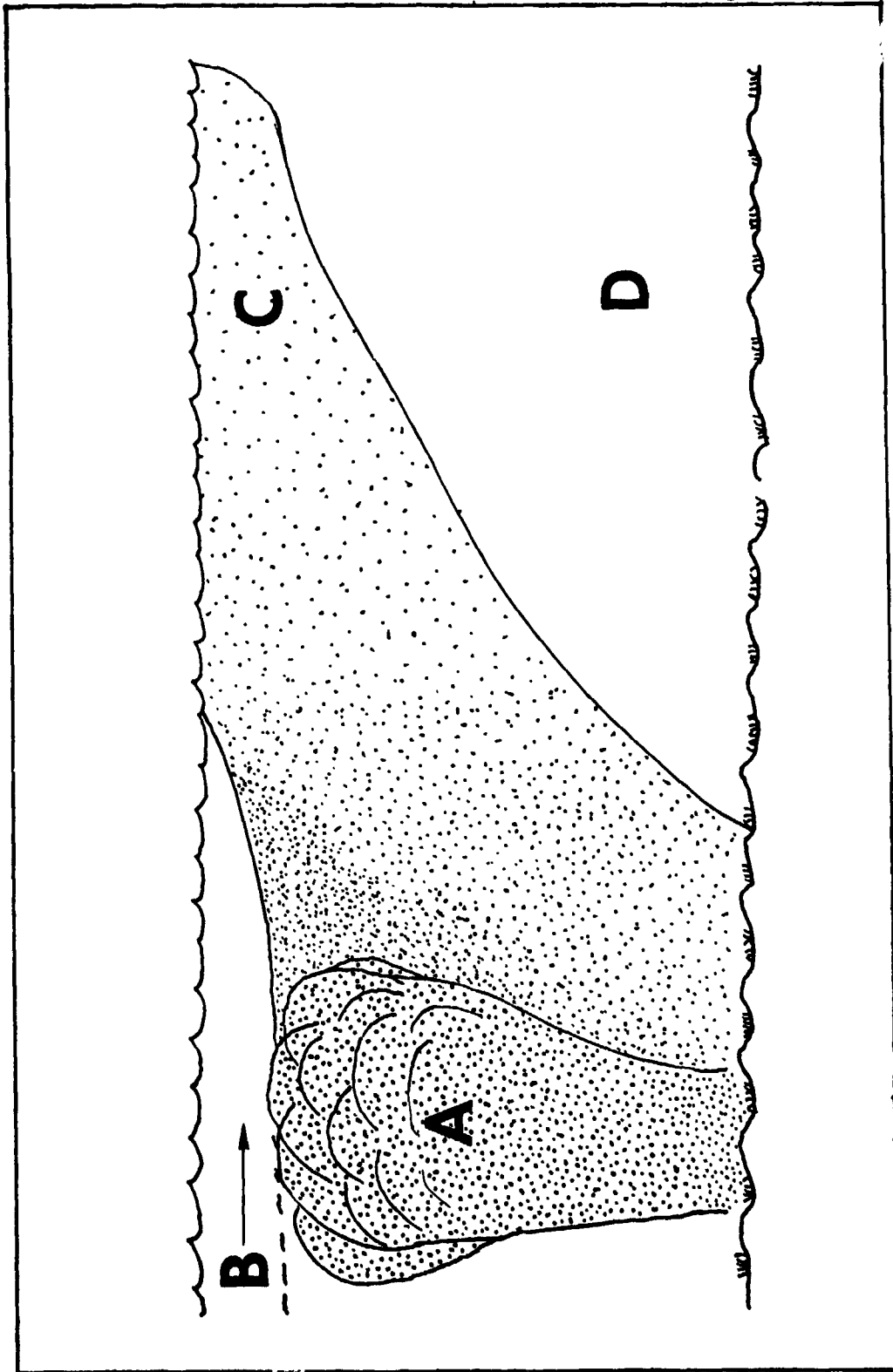


Figure 3. Hypothesized vertical shape of a whiting. (A) Source of the whiting. (B) Surface currents. (C) Tail of the whiting (D) Underlying clearer water.

CONCLUSIONS

Several points of interest were made by the investigation of these two whittings on the Little Bahama Bank.

- (1) The whittings were all elongated in form. (Figure 4).
- (2) The source areas of the whittings did not move significantly from a fixed point.
- (3) The suspended particles appeared to be evenly distributed through the vertical water column, except for a 2 m layer of clear water on the surface at the source.
- (4) They displayed definite source areas from which the sediment was dispersed in a nearly straight course by the wind and tidal current.
- (5) The whittings kept their discrete properties for long distances to the point where several whittings were observed to be parallel for relatively long distances while being separated by only 4 to 5 m or less of clear water (Figure 5). They would eventually mix.

ORIGINAL PAGE IS
OF POOR QUALITY



Fig. 4. Elongated shape of the whittings and the R/V Calypso.
(Courtesy of Joe Thompson and the Cousteau Society)



Fig. 5. Parallel courses of several distinct and separate
whittings. (Courtesy of Joe Thompson and the
Cousteau Society)

- (6) Two possible new causes of whittings have been observed:
- (a) A large school of fish, accompanied by sharks, was observed stirring up the bottom sediments in the source of the first whiting.
 - (b) Callianassa, burrowing shrimp, mounds were observed dispersing sediments to a height of a meter or more in the middle of the second whiting.
- (7) The formation of a new whiting was observed aurally from a helicopter and appeared as billowing, mushrooming sediments being presumably forced from the bottom to the surface by an as yet unexplained source.

Further sediment analyses being conducted by Ginsburg at the University of Miami will hopefully add to the knowledge obtained on the origin of these two whittings on the Little Bahama Bank. It is also hoped that these observations may generate future studies on the origin of whittings that will take into consideration the old as well as these new hypothesized sources of the aragonite particles.

ACKNOWLEDGEMENTS

This research was funded by the Environmental Research Institute of Michigan, the National Aeronautics and Space Administration and the Cousteau Society. We are grateful to the divers and crew of the Calypso who ventured into the shark-infested whittings to collect the necessary samples.

The manuscript was improved by the comments of Drs. R. Rezak and J. C. Harlan.

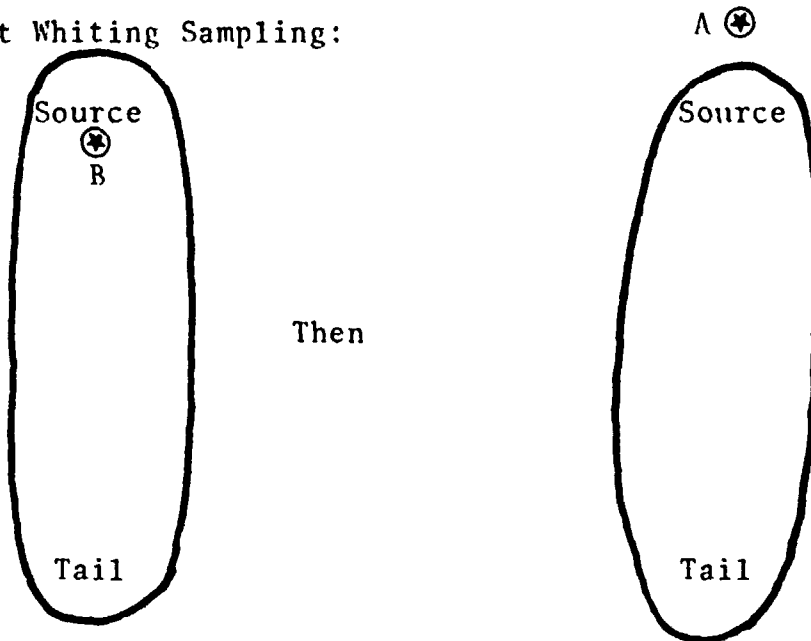
REFERENCES

- [1] Bathurst, R.G.C. (1975). Developments in sedimentology 12, carbonate sediments and their diagenesis. Elsevier Scientific Publ. Co., New York, New York.
- [2] Black, M. (1933). The precipitation of calcium carbonate on the Great Bahama Bank. *Geol. Mag.* 70, 455-466.
- [3] Broecker, W. S. and Takahashi, T. (1966). Calcium carbonate precipitation on the Bahama Banks. *J. Geophys. Res.* 71, 1575-1602.
- [4] Cloud, P. E., Jr. (1962). Environment of calcium carbonate deposition west of Andros Island, Bahamas. *U. S. Geol. Surv. Profess. Papers* 350, 1-138.
- [5] Costin, J. M. (1965). Circulation near the southern Berri Islands, Bahamas. Tech Rept. U. S. At. Energy Comm. Tech. Rept. CU-23-65, unpublished.
- [6] DeGroot, K. (1965). Inorganic precipitation of calcium carbonate from sea water. *Nature* 207, 404-405.
- [7] Ginsburg, R. N. (1956). Environmental relationships of grain size and constituent particles in some south Florida carbonate sediments. *Bull. Am. Assoc. Petrol. Geologists* 40, 2384-2427.
- [8] Ginsburg, R. N. (1957). Early diagenesis and lithification of shallow-water carbonate sediments in south Florida. In: R. J. LeBlanc and J. G. Breeding (Editors), *Regional Aspects of Carbonate Deposition Soc. Econ. Paleontologists Mineralogists, Spec. Publ.* 5, 80-99.
- [9] Katz, B. (1965). Circulation near the southern Berri Islands, Bahamas. Tech Rept. U. S. At. Energy Comm., Tech. Rept. CU-23-65, unpublished.
- [10] Lowenstan, H. A. and Epstein, S. (1957). On the origin of sedimentary aragonite needles of the Great Bahama Bank, *J. Geol.* 65, 364-375.
- [11] Neev, D. and Emery, K. O. (1967). The Dead Sea. Depositional processes and environments of evaporites. *Israel Geol. Surv. Bull.* 41, 1-147.

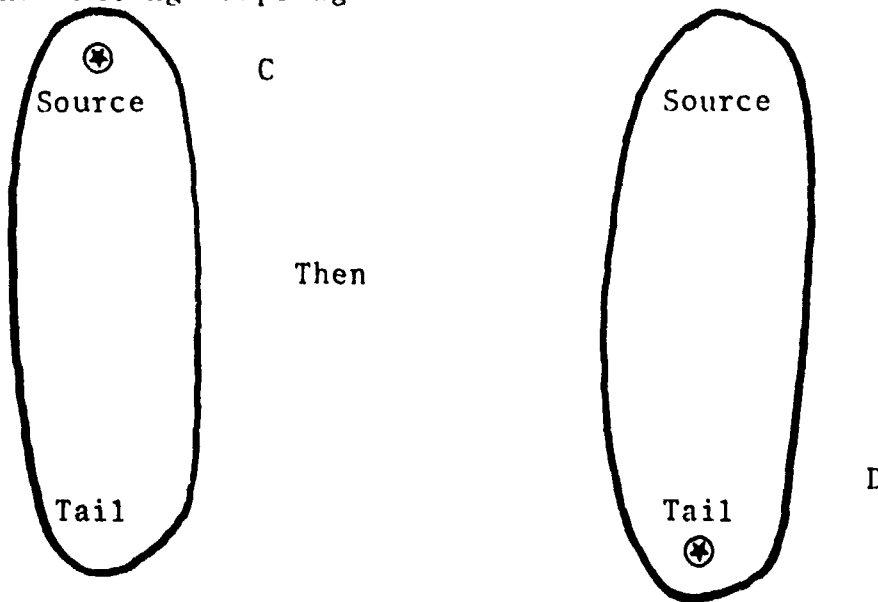
- [12] Neumann, A. C. and Land, L. S. (1969). Algal production and lime mud deposition in the Bright of Abaco: a budget. Geol. Soc. Am., Spec. Papers 121, 219 (abstract).
- [13] Revelle, R. and Fairbridge, R. (1957). Carbonates and carbon dioxide. Geol. Soc. Am., Mem. 67 (1), 239-295.
- [14] Rezak, R. (1976). Personal communications. Texas A&M University, College Station.
- [15] Shinn, E. A. (1968). Burrowing in recent lime sediments of Florida and the Bahamas. J. Paleontol. 42, 879-894.
- [16] Smith, C. L. (1940). The Great Bahama Bank.
1. General hydrographic and chemical factors.
2. Calcium carbonate precipitation. J. Marine Res. (Sear Found. Marine Res.) 3, 1-31, 147-189.
- [17] Stockman, K. W., Ginsbery, R. N. and Shinn, E. A. (1967). The production of lime mud by algae in south Florida. J. Sediment. Petrol., 37, 633-648.
- [18] Traganza, E. D. (1967). Dynamics of the carbon-dioxide system on the Great Bahama Bank. Bull. Mar. Sci. Gulf Caribbean, 17, 348-366.
- [19] Wells, A. J. and Illing, L. V. (1964). Present day precipitation of calcium carbonate in the Persian Gulf. In: L.N.J.M. Van Straaten (Editor), Deltaic and Shallow Marine Deposits. Elsevier, Amsterdam, 429-435.
- [20] Weyl, P. K. (1961). The carbonate saturometer. J. Geol. 69, 32-44.

Summary of Whiting Sampling

I. First Whiting Sampling:



II. Second Whiting Sampling:



III. One Sample 5 Miles from the Plumes (Whitings)

E ⊗

GENERAL SAMPLING INFORMATION

Zodiac (Rubber Raft) Samples:

- (1) Secchi
- (2) Sea Surface Temperature (Bucket Thermometer)
- (3) Surface Salinity Samples
- (4) Gallon Surface Water Samples

Diver Collected Samples:

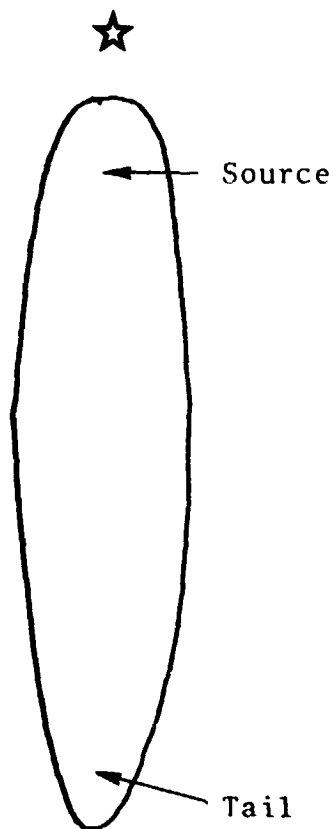
- (1) Bottom Temperature (Reversing Thermometer)
- (2) Bottom Salinity Sample
- (3) Gallon Bottom Water Samples (Niskin Bottles)
- (4) Bottom Sediment Samples
- (5) Depth
- (6) Vertical Visibility
- (7) Horizontal Visibility
- (8) Current Direction
- (9) Current Speed
- (10) General Bottom Description and Comments

Helicopter and T-38 Jet:

Spotted source and tail of whittings. Also spotted clear areas out of the plume.

DATE: 9/5/75

STATION: EA



* The samples were collected from clear waters outside of the plume or whiting #1.

Sample Code:

- (1) AT-1 Gallon Water Sample Collected From the Surface
- (2) ATS- Salinity Sample Collected From the Surface
- (3) AB-1 Gallon Water Sample Collected From the Bottom
- (4) ABS- Salinity Sample Collected From the Bottom
- (5) A,A,A-2 Sediment Sample From the Bottom

Secchi: Seen laying on the Bottom

Sea Surface Temperature: 29.94°C

Bottom Temperature: 30.21°C-(A = 33.2°C) (possible diver problem)

Depth: 7 m

Vertical Visibility: 7 m

Horizontal Visibility: 5 m

Current Direction: From SE

Current Speed: Material moved 98" in 19 seconds

Comments:

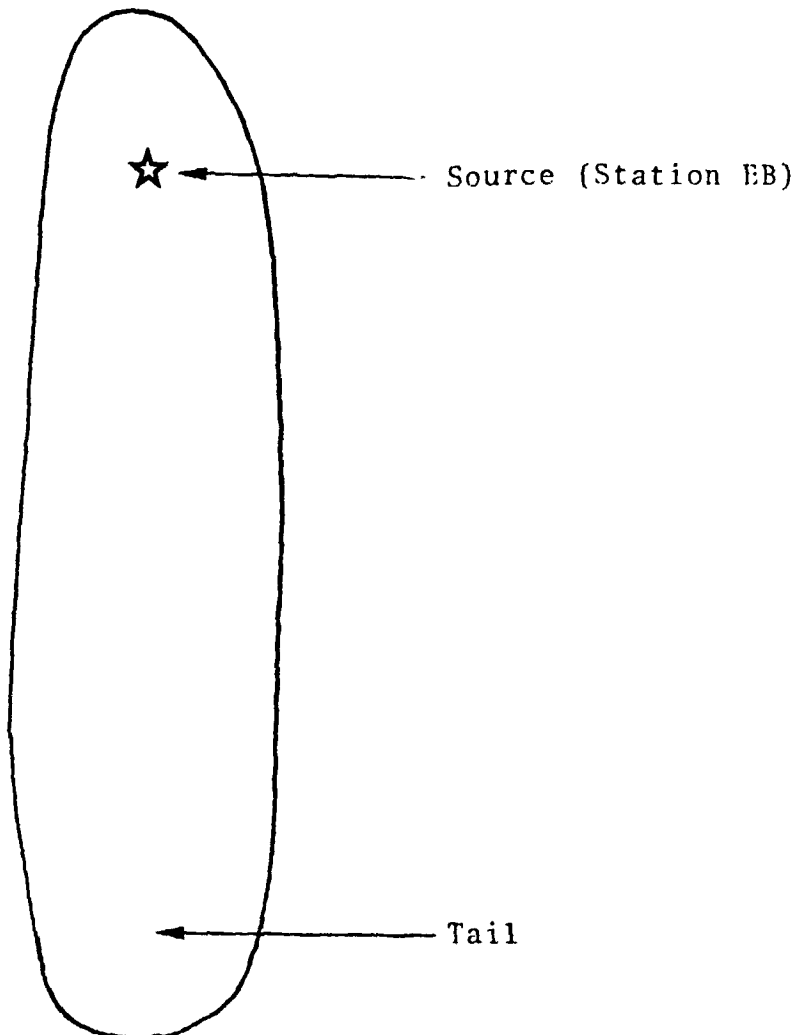
- (1) Bottom covered by mounds 4-12" high
- (2) Eel grass surrounded mounds
- (3) Three bottom samples were collected from top of mounds



- (4) No sharks were observed
- (5) On bone fish were observed
- (6) No mollusks were observed
- (7) Helicopter pilot spotted new sources that appeared to be billowing (mushrooming) clouds of sediments coming to the surface.

DATE: 9/5/75

STATION: EB (Source of First Whiting)



Sample Code:

- (1) BT-2 Gallon Samples Collected on the Surface
- (2) BTS- Salinity Sample Collected on the Surface
- (3) BB-2 Gallon Samples Collected From the Bottom
- (4) BBS- Salinity Sample Collected From the Bottom
- (5) BBB-3 Sediment Samples From the Bottom

Secchi: 7.0 m

Sea Surface Temperature: 29.93°C

Bottom Temperature: 29.92°C - (A = 30.1°C)

Depth: 7.5 m

Vertical Visibility: 2.0 meters above bottom

Horizontal Visibility: 1.5 Feet

Current Direction: No Current

Current Speed: No Current

Comments:

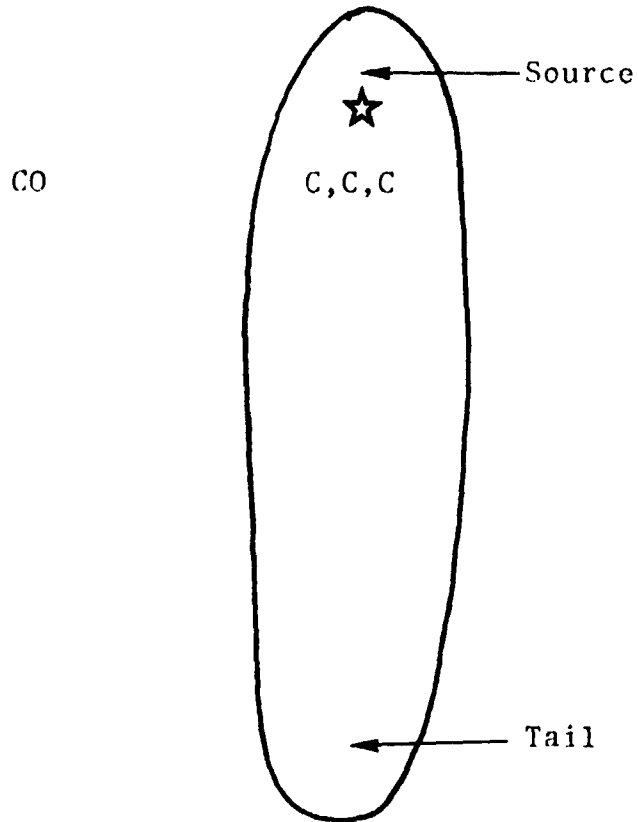
- (1) Mounds from 4 to 12 inches covered the bottom
- (2) Eel grass surrounded the mounds
- (3) Three bottom sediment samples came from the top of the mounds



- (4) Sharks were observed near the Zodiac
- (5) Bone fish in large numbers were observed hitting and bouncing off of the bottom
- (6) Mollousks were also observed by one diver to be squirting up sediments
- (7) The source was spotted by helicopter
- (8) There was a layer of relatively clear water (2 in thick) on the surface, but was turbid from 2 m to the bottom

DATE: 9/5/75

STATION: EC (Source of Second New Whiting)



Sample Code:

- (1) CT-1 Gallon water sample collected from the surface
- (2) CTS- Salinity sample collected from the surface
- (3) CB-1 Gallon water sample collected from the bottom
- (4) CBS- Salinity sample collected from the bottom
- (5) C,C,C-3 Sediment samples collected from the bottom
(See Explanation)
- (6) CO-1 Sediment sample collect from the bottom outside
of the plume

Secchi: 3.75 m

Sea Surface Temperature: 30.98°C

Bottom Temperature: 30.3°C (A - 32.3°C)

Depth: 6.5 m

Vertical Visibility: 1 m before bottom was visible

Horizontal Visibility: 2 m lateral visibility

Current Direction: From S.E.

Current Speed: 9 seconds to go 18 inches.

Comments:

- (1) Bottom covered by mounds 4 - 12" in height.
- (2) Eel grass surrounded mounds.
- (3) 2 bottom sediment samples collected from mound tops (C,C)



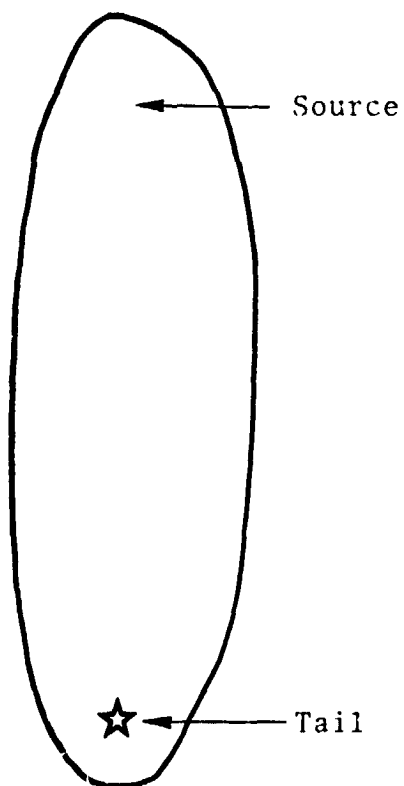
- (4) 1 bottom sediment sample collected from between mounds



- (5) No sharks were observed
- (6) No bonefish were observed
- (7) No mollusks were observed
- (8) Sediments between mounds looked muddier and darker, mound sand looked clean and white.

DATE: 9/5/75

STATION: ED (Tail of Second Plume)



Sample Code:

- (1) DT-1 Gallon Water Sample Collected From the Surface
- (2) DTS- Surface Salinity Sample
- (3) DB-1 Gallon Water Sample Collected From the Bottom
- (4) DBS- Bottom Salinity Sample
- (5) Sediment Samples:

D = From top of Mound



D+ = From Between Mounds



D++ = From Top and Bottom of Hounds



DO = From Outside of the Plume

Secchi: 4.25 m

Sea Surface Temperature: 31.2°C

Bottom Temperature: 30.20 - (30.25-A)

Depth: 7 m

Vertical Visibility: 2 m from bottom

Horizontal Visibility: 2 m

Current Direction: From SE (45°)

Comments:

- (1) Bottom covered by mounds 4-12" in height
- (2) Eel Grass surrounded mounds
- (3) Three bottom sediment samples collected
(See Previous page for sample code)
- (4) No sharks were observed
- (5) No bonefish were observed
- (6) No mollusks were observed

DATE: 9/5/75

STATION: EE

One Bottom Sediment Sample Was Collected About 5 miles
From the Sited Whiting Area.

Sediment Sample Is Marked "+++".